J|A|C|S
ARTICLES
Published on Web 03/20/2007

Coupling of Functional Hydrogen Bonds in Pyridoxal-5′-phosphate−Enzyme Model Systems Observed by Solid-State NMR Spectroscopy

Shasad Sharif,[‡] David Schagen,[‡] Michael D. Toney,[†] and Hans-Heinrich Limbach*,[‡]

Contribution from the Institut für Chemie und Biochemie, Takustrasse 3, Freie Universität Berlin, D-14195 Berlin, Germany, and the Department of Chemistry, University of California-Davis, Davis, California 95616

Received August 28, 2006; E-mail: limbach@chemie.fu-berlin.de

Abstract: We present a novel series of hydrogen-bonded, polycrystalline 1:1 complexes of Schiff base models of the cofactor pyridoxal-5′-phosphate (PLP) with carboxylic acids that mimic the cofactor in a variety of enzyme active sites. These systems contain an intramolecular OHN hydrogen bond characterized by a fast proton tautomerism as well as a strong intermolecular OHN hydrogen bond between the pyridine ring of the cofactor and the carboxylic acid. In particular, the aldenamine and aldimine Schiff bases *N*-(pyridoxylidene)tolylamine and *N*-(pyridoxylidene)methylamine, as well as their adducts, were synthesized and studied using ^{15}N CP and ^{1}H NMR techniques under static and/or MAS conditions. The geometries of the hydrogen bonds were obtained from X-ray structures, ^{1}H and ^{15}N chemical shift correlations, secondary H/D isotope effects on the ^{15}N chemical shifts, or directly by measuring the dipolar ^{2}H−^{15}N couplings of static samples of the deuterated compounds. An interesting coupling of the two "functional" OHN hydrogen bonds was observed. When the Schiff base nitrogen atoms of the adducts carry an aliphatic substituent such as in the internal and external aldimines of PLP in the enzymatic environment, protonation of the ring nitrogen shifts the proton in the intramolecular OHN hydrogen bond from the oxygen to the Schiff base nitrogen. This effect, which increases the positive charge on the nitrogen atom, has been discussed as a prerequisite for cofactor activity. This coupled proton transfer does not occur if the Schiff base nitrogen atom carries an aromatic substituent.

Introduction

Vitamin B_6 or pyridoxine (PN)[1−3] plays an important role in living systems (Scheme 1). After conversion to pyridoxal-5′-phosphate (PLP),[4,5] it is incorporated into a variety of enzymes that catalyze reactions of amino acids such as transamination, decarboxylation, and racemization.[6−9] During transamination,[10] pyridoxamine-5′-phosphate (PMP) occurs as an obligatory intermediate form of the cofactor.[11−13] According to the crystal structures of PLP-dependent enzymes,[14−18] PLP is covalently bound in their active sites as a Schiff base. Binding can occur either as an "internal aldimine" with the ϵ-amino group of a

Scheme 1. (a) Vitamin B_6: Pyridoxine (PN), (b) Pyridoxal (PL), (c) Pyridoxal Hemiacetal, (d) Pyridoxal-5′-phosphate (PLP), (e) Schiff Base, (f) Pyridoxamine-5′-phosphate (PM)

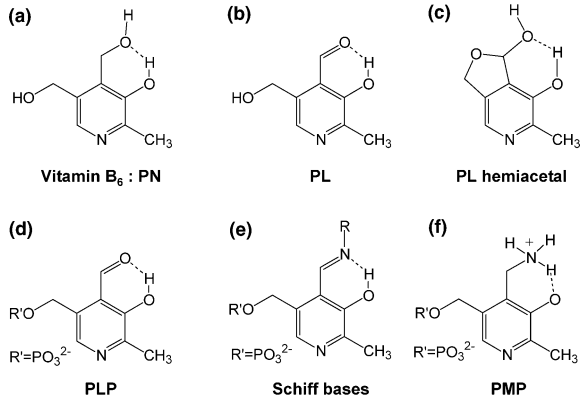

‡ Freie Universität Berlin.
† University of California−Davis.

(1) Longo, J.; Franklin, K. J.; Richardson, M. F. *Acta Crystallogr., Sect. B* **1982**, *38*, 2721−2724.
(2) Bacon, G. E.; Plant, J. S. *Acta Crystallogr., Sect. B* **1980**, *36*, 1130−1136.
(3) Hanic, F. *Acta Crystallogr.* **1966**, *21*, 332−340.
(4) Snell, E. E.; Di Mari, S. J. *The Enzymes: Kinetics and Mechanism*, 3rd ed.; Boyer, P. D., Ed.; Academic Press: New York, 1970; Vol. 2, pp 335−362.
(5) Fujiwara, T. *Bull. Chem. Soc. Jpn.* **1973**, *46*, 863−871.
(6) Christen, P.; Metzler, D. E. *Transaminases*, 1st ed.; Wiley: New York, 1985; pp 37−101.
(7) Spies, M. A.; Toney, M. D. *Biochemistry* **2003**, *42*, 5099−5107.
(8) Malashkevich, V. N.; Toney, M. D.; Jansonius, J. N. *Biochemistry* **1993**, *32*, 13451−13462.
(9) Zhou, X.; Toney, M. D. *Biochemistry* **1999**, *38*, 311−320.
(10) Snell, E. E.; Di Mari, S. J. In *The Enzymes*; Boyer, P. D., Ed.; Academic Press: New York, 1970; Vol. 2.
(11) MacLaurin, C. L.; Richardson, M. F. *Acta Crystallogr., Sect. C* **1985**, *41*, 261−263.
(12) Longo, J.; Richardson, M. F. *Acta Crystallogr., Sect. B* **1980**, *36*, 2456−2458.
(13) Giordano, F.; Mazzarella, L. *Acta Crystallogr., Sect. B* **1971**, *27*, 128−134.
(14) Jager, J.; Moser, M.; Sauder, U.; Jansonius, J. N. *J. Mol. Biol.* **1994**, *239*, 285−305.
(15) Smith, D. L.; Almo, S. C.; Toney, M. D.; Ringe, D. *Biochemistry* **1989**, *28*, 8161−8167.
(16) Shaw, J. P.; Petsko, G. A.; Ringe, D. *Biochemistry* **1997**, *36*, 1329−1342.
(17) Stamper, C. G. F.; Morollo, A. A.; Ringe, D. *Biochemistry* **1998**, *37*, 10438−10445.
(18) Jansonius, J. N. *Curr. Opin. Struct. Biol.* **1998**, *8*, 759−769.

10.1021/ja066240h CCC: $37.00

Scheme 2. Overview of the First Step of the Catalytic Cycle

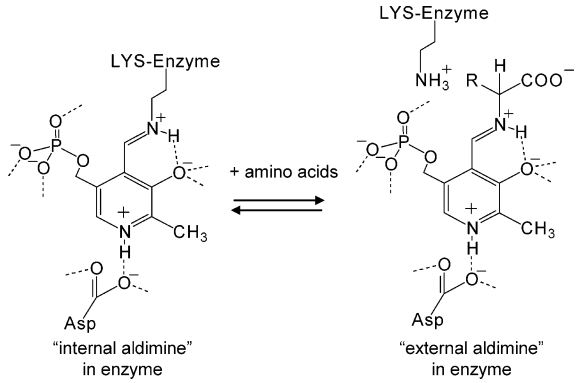

lysine residue or as or an "external aldimine" with the amino acid substrate (Scheme 2). Both aldimines are stabilized by an intramolecular OHN hydrogen bond. The ring nitrogen is involved in an intermolecular OHN hydrogen bond with an aspartic acid side chain in many PLP-dependent enzymes. The phosphate group contributes to PLP binding by hydrogen bonding but plays no direct role in the mechanism.

The protonation states of the two functional OHN hydrogen bonds have a large influence on enzymatic function.[4,6] In the first step of the catalytic cycle, it is assumed that the bridging proton of the intramolecular OHN hydrogen bond has to be transferred from the phenolic oxygen to the imino nitrogen, a process which may be assisted by protonation of the pyridine ring (Scheme 2).[6,19]

In order to elucidate the properties of the intramolecular OHN hydrogen bond, model studies have been reported for several Schiff bases of aromatic *ortho*-hydroxylaldehydes dissolved in organic liquids or embedded in the organic solid state.[20−27] Using UV−vis,[28] ^{13}C,[29,30] ^{17}O,[31,32] and ^{15}N[20,33] NMR spectroscopy, it has been shown that these compounds exhibit a keto−enol tautomerism between the enolimine form (OH form) and the ketoamine form (HN form) that interconverts very rapidly via proton transfers, as illustrated in Scheme 3. Many factors, such as the local polarity and specific solvation, influence this equilibrium.[20] In particular, the analysis of the ^{15}N chemical shifts δ(OHN) provides information about the equilibrium constants of the tautomerism. On the other hand, in order to

Scheme 3. Schematic View of the Keto−Enol Tautomerism of the Aldenamine Schiff Base (R = Tolyl) and Aldimine Schiff Base ($R = CH_3$) and the Influence of Protonation of the Pyridine Nitrogen. Only the Zwitterionic Resonance Structure is Shown for Tautomer *b*

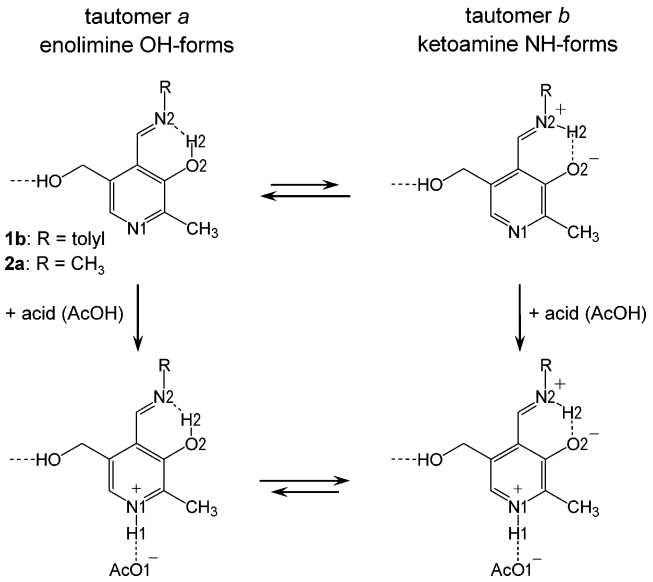

model the intermolecular OHN hydrogen bond, some of us have studied various acid-pyridine or 2,4,6-trimethylpyridine (collidine) complexes using liquid- and solid-state NMR techniques.[34−44] Hydrogen bond geometries were obtained as a function of the position of the proton in the bridge. Moreover, solvent effects on the intermolecular OHN hydrogen bond geometries were studied.[45]

However, the interaction between the functional OHN hydrogen bonds is still open to debate. Therefore, using solid state ^1H and ^{15}N MAS NMR techniques, we have examined the coupling between these hydrogen bonds. This necessitated the design of ^{15}N-labeled model Schiff bases that mimic the interactions of PLP in enzyme active sites. As the phosphate group is not directly involved in the mechanisms of PLP-catalyzed reactions, we prepared the singly and doubly ^{15}N-labeled Schiff bases **1b** (R = tolyl, aldenamine) and **2a** (R = methyl, aldimine) of pyridoxal[11] (PL) to vary the basicity of the imino nitrogen, as illustrated in Scheme 3. Several novel 1:1 acid-base complexes of benzoic acid derivatives with these

(19) Bach, R. D.; Canepa, C. *J. Am. Chem. Soc.* **1997**, *119*, 11725−11733.
(20) Sharif, S.; Denisov, G. S.; Toney, M. D.; Limbach H. H. *J. Am. Chem. Soc.* **2006**, *128*, 3375−3387.
(21) Benedict, C.; Langer, U.; Limbach, H. H.; Ogata, H.; Takeda, S. *Ber. Bunsen-Ges. Phys. Chem.* **1998**, *102*, 335−339.
(22) Hansen, P. E.; Sitkowski, J.; Stefaniak, L.; Rozwadowski, Z.; Dziembowska, T. *Ber. Bunsen-Ges. Phys. Chem.* **1998**, *102*, 410−413.
(23) Rozwadowski, Z.; Majewski, E.; Dziembowska, T.; Hansen, P. E. *J. Chem. Soc., Perkin Trans. 2* **1999**, 2809−2817.
(24) Schilf, W.; Kamienski, B.; Dziembowska, T.; Rozwadowski, Z.; Szady-Chelmieniecka, A. *J. Mol. Struct.* **2000**, *552*, 33−37.
(25) Kamienski, B.; Schilf, W.; Dziembowska, T.; Rozwadowski, Z.; Szady-Chelmieniecka, A. *Solid State Nucl. Magn. Reson.* **2000**, *16*, 285−289.
(26) Rozwadowski, Z.; Ambroziak, K.; Szypa, M.; Jagodzinska, E.; Spychaj, S.; Schilf, W.; Kamienski, B. *J. Mol. Struct.* **2005**, *734*, 137−142.
(27) Harbison, G. S.; Roberts, J. E.; Herzfeld, J.; Griffin, R. G. *J. Am. Chem. Soc.* **1988**, *110*, 7221−7223.
(28) Rospenk, M.; Krol-Starzomska, I.; Filarowski, A.; Koll, A. *Chem. Phys.* **2003**, *287*, 113−124.
(29) Filarowski, A.; Koll, A.; Rospenk, M.; Krol-Starzomska, I.; Hansen, P. E. *J. Phys. Chem. A* **2005**, *109*, 4464−4473.
(30) Rozwadowski, Z.; Dziembowska, T. *Magn. Reson. Chem.* **1999**, *37*, 274−278.
(31) Zhuo, J. C. *Magn. Reson. Chem.* **1999**, *37*, 259−268.
(32) Kozerski, L.; Kawecki, R.; Krajewski, P.; Kwiecien, B.; Boykin, D. W.; Bolvig, S.; Hansen, P. E. *Magn. Reson. Chem.* **1998**, *36*, 921−928.
(33) Dziembowska, T.; Rozwadowski, Z.; Filarowski, A.; Hansen, P. E. *Magn. Reson. Chem.* **2001**, *39*, 67−80.
(34) Benedict, H.; Limbach, H. H.; Wehlan, M.; Fehlhammer, W. P.; Golubev, N. S.; Janoschek, R. *J. Am. Chem. Soc.* **1998**, *120*, 2939−2950.
(35) Lorente, P.; Shenderovich, I. G.; Golubev, N. S.; Denisov, G. S.; Buntkowsky, G.; Limbach, H. H. *Magn. Reson. Chem.* **2001**, *39*, 18−29.
(36) Smirnov, S. N.; Golubev, N. S.; Denisov, G. S.; Benedict, H.; Schah-Mohammedi, P.; Limbach, H. H. *J. Am. Chem. Soc.* **1996**, *118*, 4094−4101.
(37) Smirnov, S. N.; Benedict, H.; Golubev, N. S.; Denisov, G. S.; Kreevoy, M. M.; Schowen, R. L.; Limbach, H. H. *Can. J. Chem.* **1999**, *77*, 943−949.
(38) Shenderovich, I. G.; Tolstoy, P. M.; Golubev, N. S.; Smirnov, S. N.; Denisov, G. S.; Limbach, H. H. *J. Am. Chem. Soc.* **2003**, *125*, 11710−11720.
(39) Limbach, H. H.; Pietrzak, M.; Benedict, H.; Tolstoy, P. M.; Golubev, N. S.; Denisov, G. S. *J. Mol. Struct.* **2004**, *706*, 115−119.
(40) Limbach, H. H.; Pietrzak, M.; Sharif, S.; Tolstoy, P. M.; Shenderovich, I. G.; Smirnov, S. N.; Golubev, N. S.; Denisov, G. S. *Chem.−Eur. J.* **2004**, *10*, 5195−5204.
(41) Shenderovich, I. G.; Buntkowsky, G.; Schreiber, A.; Gedat, E.; Sharif, S.; Albrecht, J.; Golubev, N. S.; Findenegg, G. H.; Limbach, H. H. *J. Phys. Chem. B* **2003**, *107*, 11924−11939.
(42) Del Bene, J. E.; Elguero, J. *J. Phys. Chem. A* **2006**, *110*, 1128−1133.
(43) Del Bene, J. E.; Elguero, J. *J. Phys. Chem. A* **2005**, *109*, 10759−10769.
(44) Del Bene, J. E.; Elguero, J. *J. Phys. Chem. A* **2005**, *109*, 10753−10758.
(45) Tolstoy, P. M.; Smirnov, S. N.; Shenderovich, I. G.; Golubev, N. S.; Denisov, G. S.; Limbach, H. H. *J. Mol. Struct.* **2004**, *700*, 19−27.

Scheme 4. (a) Aldenamine Schiff Base and its Derivatives Studied in this Paper. (b) Aldimine Schiff Base and its Derivatives Studied in this Paper

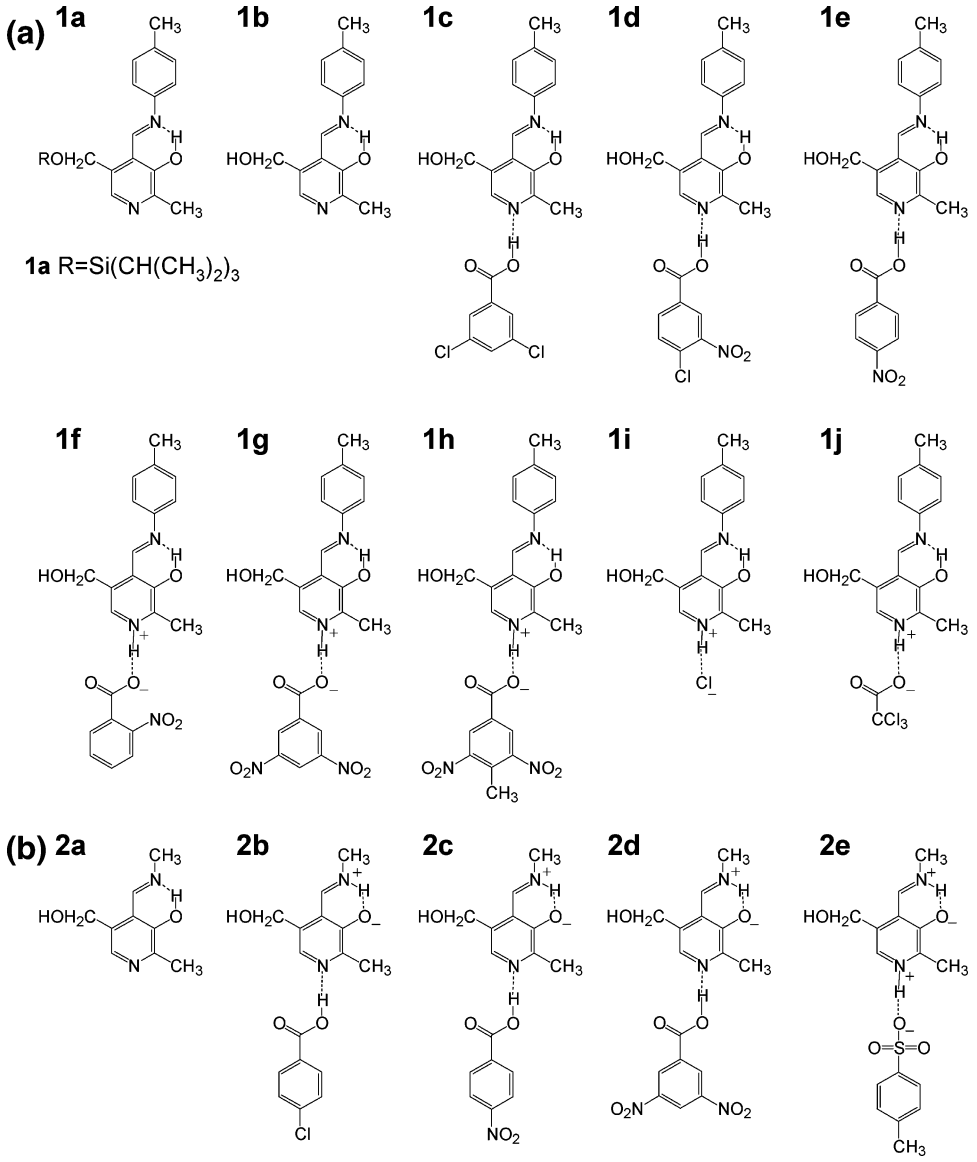

Schiff bases were designed (Scheme 4). In previous studies, some of these complexes (i.e., **1b**, **2a**, and their adducts with 2-nitrobenzoic acid **1f** and 4-nitrobenzoic acid **2c**) were investigated using X-ray crystallography.[46]

Experimental Section

A. NMR Measurements. Solid-state ^{15}N NMR spectra of ^{15}N-labeled **1a**−**1j** and **2a**−**2e** were measured at 30.41 MHz using a Bruker MSL 300 spectrometer (7 T) equipped with a 5 mm Chemagnetics MAS probe. The ^{1}H spectra were recorded on a Varian Infinity Plus 600 MHz (14 T) solid-state NMR spectrometer. Standard cross-polarization ^{15}N {^{1}H} CP NMR experiments were performed under static or magic angle spinning (MAS) conditions. In the latter case, the spinning rates were about 6 kHz. The 90° pulse width was about 8 μs, the cross-polarization contact times were 3 ms, and the recycle times were 20 s. All ^{15}N spectra are referenced to external solid ammonium chloride, $^{15}NH_4Cl$ (95% ^{15}N-enriched). Standard ^{1}H ECHO MAS NMR experiments were performed at a spinning rate of 24 kHz. The 90 and 180° pulse widths were 2 and 4 μs, respectively, using an echo delay of 20 rotor periods and a recycle time of 10 s. All ^{1}H spectra were referenced to an external sodium salt of trimethylsilylpropionic acid (TSP).

The static ^{15}N CP powder spectra of **1g**, **1i**, **1j**, and their deuterated analogues were calculated as described previously for other systems,[34,35] using procedures described by Hoelger et al.[47] From the ^{2}H−^{15}N dipolar couplings, mean cubic ND distances were derived. The distances were not corrected for vibrational averaging. One needs to distinguish between temperature effects arising from the population of excited vibrational states and anharmonic vibrational effects, which are operative also in the vibrational ground state. It is difficult to take these effects quantitatively into account. In a case where the anharmonic vibrational ground state wave function was known, an error of the ND distances of a few percent was calculated.[34] Therefore, vibrational averaging effects were neglected in this study.

B. Materials. ^{15}N-labeled pyridoxine (PN), pyridoxamine (PM), pyridoxal-5′-phosphate (PLP), pyridoxal (PL), *N*-(pyridoxylidene)-tolylamine (**1b**) (**1a** is the protected 5′-triisopropylsilyl ether of **1b**), *N*-(pyridoxylidene)methylamine (**2a**), and *p*-toluidine were synthesized from 98% ^{15}N-enriched $^{15}NH_4Cl$ (Deutero GmbH), 95% ^{15}N-enriched

(46) Sharif, S.; Powell, D. R.; Schagen, D.; Steiner, T.; Toney, M. D.; Fogle, E.; Limbach, H. H. *Acta Crystallogr., Sect. B* **2006**, *62*, 480−487.

(47) Hoelger, C. G.; Limbach, H. H. *J. Phys. Chem.* **1994**, *98*, 11803−11810.

Scheme 5. Overview of the Synthetic Route

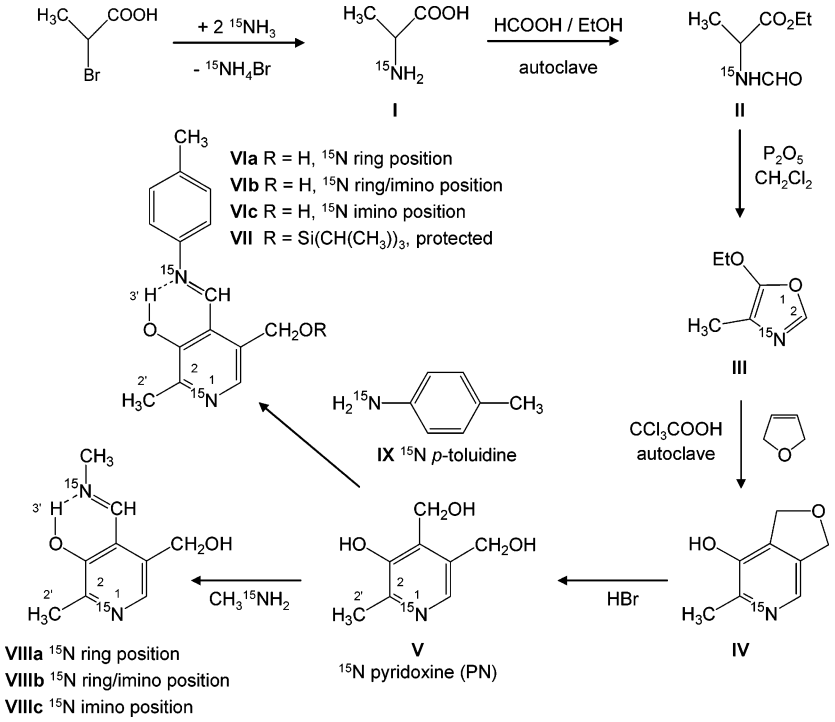

methylamine hydrochloride (Chemotrade), and/or 95% ^{15}N-enriched hydroxylamine hydrochloride (Chemotrade). 3,5-Dichlorobenzoic acid, 3-nitro-4-chlorobenzoic acid, 4-nitrobenzoic acid, 2-nitrobenzoic acid, 3,5-dinitrobenzoic acid, 3,5-dinitro-4-methylbenzoic acid, hydrochloric acid, trichloroacetic acid, 4-chlorobenzoic acid, 4-tolylsulfonic acid, pyridoxamine dihydrochloride, PLP, and pyridoxal hydrochloride were purchased from Aldrich. The following deuterated solvents were purchased from Deutero GmbH: deuteriumoxide (D_2O), dichloromethane-d_2, dimethylsulfoxide-d_6 (DMSO), methanol-d_1/-d_4, chloroform-d_1, and DCl solution in D_2O.

C. Syntheses. The synthesis of ^{15}N-labeled PN, Schiff bases ^{15}N-labeled at different positions, and PLP and its analogues is depicted in Scheme 5. As a starting point, the ^{15}N-labeled amino acid D,L-alanine (**I**) was prepared using a halogen exchange of 2-bromopropionic acid with ammonia, $^{15}NH_3$. Instead of the established methods[48−50] for preparing ^{15}N-labeled amino acids, a method described by Block[51] for unlabeled amino acids was employed. The ^{15}N-labeled **I** reacts with formic acid in ethanolic solution in an autoclave to give ethyl-*N*-formyl-D,L-alaninate (**II**); the preparation procedure followed the description by Maeda et al.[52] The dehydration of **II** to 5-ethoxy-4-methyloxazole (**III**) can be obtained using different methods;[53−55] we employed the last method using phosphorus pentoxide to give ^{15}N-labeled **III**. The reaction of **III** with 2,5-dihydrofuran catalyzed by trichloroacetic acid in a autoclave gave ^{15}N-labeled 2-methyl-3-hydroxy-4,5-epoxydimethylpyridine (**IV**).[55] The cleavage of the epoxydimethyl group, using 48% hydrobromic acid, forms the dibromide hydrobromide of PN, which was hydrolyzed to pyridoxine hydrobromide.[56,57] The pyridoxine hydrobromide was converted to pyridoxine hydrochloride (**V**) using silver chloride.[56,57] After the neutralization of pyridoxine hydrochloride, it was purified by column chromatography. The ^{15}N-ring-labeled aldenamine Schiff base (**VIa**) was prepared by oxidization of ^{15}N-labeled **V** with manganese dioxide to PL, followed by reaction with *p*-toluidine according to the method of Iwanami.[58] Using the ^{15}N-labeled *p*-toluidine (**IX**),[59,60] the ^{15}N-doubly-labeled **VIb** was accessible. The direct reaction of PL and ^{15}N-labeled *p*-toluidine (**IX**) forms the ^{15}N-imino-labeled **VIc**. In addition, the 5′-hydroxyl group of the aldenamine Schiff base was protected by the formation of the 5′-triisopropylsilyl ether,[61,62] leading to the protected ^{15}N-labeled **VII**. The aldimine Schiff base was prepared by condensation of methylamine and ^{15}N-labeled **V**, which was oxidized to PL and then transformed to ring ^{15}N-labeled **VIIIa**; the doubly ^{15}N-labeled **VIIIb** was accessible by using the ^{15}N-labeled methylamine. The ^{15}N-imino-labeled **VIIIb** was obtained by condensing PL with ^{15}N-labeled methylamine hydrochloride in aqueous solution, following the unlabeled preparation.[63−66] The 5′-triisopropylsilyl ether of the aldimine Schiff base was unstable.

^{15}N-labeled PM (**X**) was prepared from ^{15}N-enriched hydroxylamine hydrochloride according to the procedures described in refs 67−70. After acidification of the ^{15}N-labeled aldimine Schiff base, ^{15}N-labeled PL (**XI**) was obtained. The ^{15}N-labeled cofactor PLP (**XII**) was made

(48) Baumgartner, F. J.; Barrio, J. R.; Henze, E.; Schelbert, H. R.; MacDonald, N. S.; Phelps, M. E.; Kuhl, D. E. *J. Med. Chem.* **1981**, *24*, 764−766.
(49) Ogo, S.; Uehara, K.; Abura, T.; Fukuzumi, S. *J. Am. Chem. Soc.* **2004**, *126*, 3020−3021.
(50) Dimitrijevich, S. D.; Scanlon, M. D.; Anbar, M. *J. Labelled Compd. Radiopharm.* **1982**, *19*, 573−584.
(51) Block, R. J. *Chem. Rev.* **1946**, *38*, 501−571.
(52) Maeda, I.; Asai, S.; Miyashiki, H.; Yoshida, R. *Bull. Chem. Soc. Jpn.* **1972**, *45*, 1917−1918.
(53) Maeda, I.; Togo, K.; Yoshida, R. *Bull. Chem. Soc. Jpn.* **1971**, *44*, 1407−1410.
(54) Maeda, I.; Takehara, M.; Togo, K.; Asai, S.; Yoshida, R. *Bull. Chem. Soc. Jpn.* **1969**, *42*, 1435−1437.
(55) Harris, E. E.; Firestone, R. A.; Pfister, K., III; Boettcher, R. R.; Cross, F. J.; Curie, R. B.; Monaco, M.; Peterson, E. R.; Reuter, W. *J. Org. Chem.* **1962**, *27*, 2705−2706.
(56) Harris, S. A.; Folkers, K. *J. Am. Chem. Soc.* **1939**, *61*, 3307−3310.
(57) Harris, S. A.; Folkers, K. *J. Am. Chem. Soc.* **1939**, *61*, 1245−1247.
(58) Iwanami, M.; Numata, T.; Murakami, M. *Bull. Chem. Soc. Jpn.* **1968**, *41*, 161−165.
(59) Lewis, E. S.; Holliday, R. E. *J. Am. Chem. Soc.* **1969**, *91*, 426−430.
(60) Lewis, E. S.; Insole, J. M. *J. Am. Chem. Soc.* **1964**, *86*, 32−34.
(61) Corey, E. J.; Venkateswarlu, A. *J. Am. Chem. Soc.* **1972**, *94*, 6190−6191.
(62) Cunico, R. F.; Bedell, L. *J. Org. Chem.* **1980**, *45*, 4797−4798.
(63) Van Genderen, M. H. P.; Van Lier, P. M.; Buck, H. M. *Recl. Trav. Chim. Pays-Bas* **1989**, *108*, 418−420.
(64) Heyl, D.; Luz, E.; Harris, S. A.; Folkers, K. *J. Am. Chem. Soc.* **1952**, *74*, 414−416.
(65) Heyl, D.; Luz, E.; Harris, S. A.; Folkers, K. *J. Am. Chem. Soc.* **1948**, *70*, 3669−3671.
(66) Metzler, D. E. *J. Am. Chem. Soc.* **1957**, *79*, 485−490.
(67) Tanenbaum, S. W. *J. Biol. Chem.* **1956**, *218*, 733−743.
(68) Harris, S. A.; Heyl, D.; Folkers, K. *J. Am. Chem. Soc.* **1944**, *66*, 2088−2092.
(69) Ikawa, M.; Snell, E. E. *J. Am. Chem. Soc.* **1954**, *76*, 637−638.
(70) Heyl, D. *J. Am. Chem. Soc.* **1948**, *70*, 3434−3436.

by phosphorylation of the 5′-hydroxyl group of ^{15}N-labeled **VIa**[71−73] with phosphorus pentoxide in phosphoric acid. It was purified with a cation exchange column. The procedures for obtaining the unlabeled Schiff bases were described previously.[46]

1. ^{15}N-Labeled d,l-Alanine (2-Aminopropionic acid) (I). Eight grams (52 mmol) of 2-bromopropionic acid was dissolved in 250 mL of water by adding an approximately 20% solution of $^{15}NH_3$[74] in water. The product reacted positive to the ninhydrin test for the presence of amino groups (1% in water, followed by heating). Yield: 3.0 g (64%). ^{1}H NMR (500 MHz, D_2O, room temperature) (ppm/TMS): δ 1.50 (dd, $^3J(^1H,^1H) = 7.0$ Hz, $^3J(^{15}N,^1H) = 3.0$ Hz, 3H, −C$\underline{H}_3$), 3.8 (q, $^3J(^1H,^1H) = 7$ Hz, 1H, −C$\underline{H}$−). ^{13}C {^{1}H} NMR (125 MHz, D_2O, room temperature) (ppm/TMS): δ 16.40 (s, −$\underline{C}H_3$), 50.74 (d, −$\underline{C}$H−, $^1J(^{15}N,^{13}C) = 5.6$ Hz), 175.95 (s, −$\underline{C}$OOH).

2. ^{15}N-Labeled Ethyl-*N*-formyl-d,l-alaninate (II). A mixture of 4 g (45 mmol) of ^{15}N-labeled d,L-alanine (**I**), 6.3 g (137 mmol) of abs formic acid, and 140 mL of abs ethanol was allowed to react in an autoclave at 220 °C overnight and was then chilled in an ice bath. The ethanol and water formed in the reaction were distilled off under reduced pressure. Next, 140 mL of ethanol was added to the residue and removed under reduced pressure. This treatment was repeated three times. The residue was distilled in a bulb tube at 80−100 °C and 0.3 mbar. The product was stored under inert gas at −23 °C. Yield: 3.3 g (50%). ^{1}H NMR (500 MHz, $CDCl_3$, room temperature) (ppm/TMS): δ 1.27 (t, $^3J(^1H,^1H) = 7.2$ Hz, 3H, −CH$_2$−C$\underline{H}_3$), 1.42 (dd, $^3J(^1H,^1H) = 7.2$, $^3J(^{15}N,^1H) = 2.7$ Hz, 3H, −C$\underline{H}_3$), 4.20 (q, $^3J(^1H,^1H) = 7.2$ Hz, 2H, −C$\underline{H}_2$−CH$_3$), 4.60 (q, $^3J(^1H,^1H) = 7.2$ Hz, 1H, −C$\underline{H}$−), 6.52 (ddd, $^1J(^{15}N,^1H) = 92.0$, ^3J(H,^{1}H) = 7.6, $^3J(^1H,^1H) = 1.6$ Hz, 1H, $\underline{H}$N), 8.16 (d, $^2J(^{15}N,^1H) = 16.1$ Hz, 1H, −C$\underline{H}$O). ^{13}C {^{1}H} NMR (125 MHz, $CDCl_3$, room temperature) (ppm/TMS): δ 14.24 (s, −CH$_2$−$\underline{C}$H$_3$), 18.62 (s, −$\underline{C}$H$_3$), 47.06 (d, $^1J(^{15}N,^{13}C) = 11.7$ Hz, −$\underline{C}$H−), 61.87 (s, −$\underline{C}$H$_2$−), 160.82 (d, $^1J(^{15}N,^{13}C) = 13.37$ Hz, −$\underline{C}$HO), 172.81 (s, −$\underline{C}$OOH).

3. ^{15}N-Labeled 5-Ethoxy-4-methyloxazole (III). Freshly prepared (4 g; 27 mmol) ^{15}N-labeled ethyl-*N*-formyl-**d,l**-alaninate (**II**) was dissolved in 250 mL of dist dichloromethane, and 17 g of P_2O_5 was added slowly. The reaction mixture was heated for 24 h under reflux. The solution was chilled to 0 °C, and 250 mL of 20% aqueous NaOH was slowly added. The suspension was extracted four times with 300 mL of dichloromethane and dried over $NaHCO_3$; the solvent was removed under reduced pressure. The residue was distilled in a bulb tube at 39 °C and 25 mbar. The product was stored under inert gas at −23 °C. Yield: 2.7 g (78%). ^{1}H NMR (500 MHz, $CDCl_3$, room temperature) (ppm/TMS): δ 1.34 (t, $^3J(^1H,^1H) = 7.1$ Hz, 3H, −CH$_2$−C$\underline{H}_3$), 2.03 (d, $^3J(^{15}N,^1H) = 2.3$ Hz, 3H, −C$\underline{H}_3$), 4.15 (q, $^3J(^1H,^1H) = 7.1$ Hz, 2H, −C$\underline{H}_2$−CH$_3$), 7.37 (d, $^2J(^{15}N,^1H) = 12.6$ Hz, 1H, −C$\underline{H}$). ^{13}C {^{1}H} NMR (125 MHz, $CDCl_3$, room temperature) (ppm/TMS): δ 10.18 (d, $^2J(^{15}N,^{13}C) = 6.4$ Hz, −C$\underline{H}_3$), 15.19 (s, −CH$_2$−$\underline{C}$H$_3$), 70.32 (s, −$\underline{C}$H$_2$−), 112.5 (d, $^1J(^{15}N,^{13}C) = 1.6$ Hz, $\underline{C}$4), 142.36 (d, $^1J(^{15}N,^{13}C) = 1.2$ Hz, $\underline{C}$2), 154.56 (d, $^2J(^{15}N,^{13}C) = 0.9$ Hz, $\underline{C}$5).

4. ^{15}N-Labeled 2-Methyl-3-hydroxy-4,5-epoxydimethylpyridine (IV). A solution of freshly prepared, 2.5 g (20 mmol) of ^{15}N-labeled 5-ethoxy-4-methyloxazole (**III**) in a 20-fold molar excess of 2,5-dihydrofuran containing 1% trichloroacetic acid was heated in an autoclave for 5 h at 190 °C. After cooling to room temperature overnight, the precipitate was washed with diethylether. Excess 2,5-dihydrofurane was removed under high vacuum, and the product was purified by column chromatography (silica, CH_2Cl_2/MeOH, 10:1). Yield: 1.9 g (63%). ^{1}H NMR (500 MHz, CD_3OD, room temperature) (ppm/TMS): δ 2.42 (d, $^3J(^{15}N,^1H) = 3.0$ Hz, 3H, −C$\underline{H}_3$), 5.05 (m, 4H, −C$\underline{H}_2$−), 7.77 (d, $^2J(^{15}N,^1H) = 9.2$ Hz, 1H, C$\underline{H}$).

5. ^{15}N-Labeled Pyridoxine (PN) (V). A solution containing 1.9 g (12 mmol) of ^{15}N-labeled 2-methyl-3-hydroxy-4,5-epoxydimethylpyridine (**IV**) in 12 mL of 48% hydrobromic acid was heated under reflux for 1 h. Upon cooling in ice water, crystals separated and were filtered and washed with diethylether. The hydrochloride was prepared by boiling the hydrobromide for 30 min in 100 mL of water and removing the bromide ions with freshly prepared silver chloride. The filtrate was evaporated to dryness. The pyridoxine hydrochloride was purified by column chromatography (silica, CH_2Cl_2/CH_3OH, 10:1). The product was checked by mass spectroscopy, and the ^{15}N isotopic enrichment was estimated as >90%. Yield: 2.1 g (84%). ^{1}H NMR (500 MHz, D_2O, room temperature) (ppm/TMS): δ 2.65 (d, $^2J(^{15}N,^1H) = 3.2$ Hz, 3H, 2′-C$\underline{H}_3$), 4.81 (s, 2H, 5′-C$\underline{H}_2$−), 5.01 (s, 2H, 4′-C$\underline{H}_2$−), 8.17 (d, $^2J(^{15}N,^1H) = 3.2$ Hz, 1H, 6-C$\underline{H}$). ^{13}C {^{1}H} NMR (125 MHz, D_2O, room temperature) (ppm/TMS): δ 14.56 (s, 2′-$\underline{C}$H$_3$), 57.00 (s, 4′-$\underline{C}$H$_2$−), 58.3 (s, 5′-$\underline{C}$H$_2$−), 130.00 (d, $^1J(^{15}N,^{13}C) = 12.7$ Hz, $\underline{C}$6), 136.96 (s, $\underline{C}$5), 140.79 (s, $\underline{C}$4), 142.95 (d, $^1J(^{15}N,^{13}C) = 14.4$ Hz, $\underline{C}$2), 152.93 (s, $\underline{C}$3). These ^{13}C NMR data are similar to those reported previously for unlabeled pyridoxine.[75,76]

6. ^{15}N-Labeled (Ring and Doubly) *N*-(Pyridoxylidene)tolylamine (VIa,b). For preparation of the ring or doubly ^{15}N-labeled product, 0.4 g (1.9 mmol) of ^{15}N-labeled pyridoxine hydrochloride (**V**) in aqueous solution was added to MnO_2 that was freshly prepared from 0.3 g of potassium permanganate, 0.4 g of sodium bisulfite $NaHSO_3$, and 1 mL of 50% sulfuric acid in 20 mL of water. The solution was stirred for 4 h after adding 0.3 g (2.2 mmol) of *p*-toluidine and/or ^{15}N-labeled *p*-toluidine (**IX**). After diluting the solution to 400 mL with water, the pH was adjusted with 1 M $NaHCO_3$ solution to 7.5. The Schiff base that precipitated from solution was filtered and washed with water. The product was dried under vacuum. By using unlabeled *p*-toluidine, the singly ring ^{15}N-labeled Schiff base was obtained. Yield: 0.18 g (37%). **VIa** (^{15}N-ring-labeled): ^{1}H NMR (500 MHz, DMSO-d_6, room temperature) (ppm/TMS): δ 2.36 (s, 3H, Ar−C$\underline{H}_3$), 2.43 (d, 3H, $^2J(^{15}N,^1H) = 2.9$ Hz, 2′-C$\underline{H}_3$), 4.77 (d, 2H, $^3J(^1H,^1H) = 5.5$ Hz, 5′-C$\underline{H}_2$−), 5.42 (t, 1H, $^3J(^1H,^1H) = 5.5$ Hz, 5″-O$\underline{H}$), 7.30−7.45 (m, 4H, −C$_6\underline{H}_4$−), 7.99 (d, 1H, $^2J(^{15}N,^1H) = 11.0$ Hz, $\underline{H}$6), 9.18 (s, 1H, $\underline{H}$4′), 14.06 (s, 1H, $\underline{H}$3′).

7. ^{15}N-Labeled (Imino) *N*-(Pyridoxylidene)tolylamine (VIc). The imino ^{15}N-labeled product was prepared as follows. An aqueous solution of 0.37 g (2.2 mmol) of pyridoxal hydrochloride was added to 0.3 g (2.2 mmol) of ^{15}N-labeled *p*-toluidine (**IX**). The resulting mixture was brought to a pH 7.5 by adding 1 M $NaHCO_3$ solution. The mixture was kept on ice for 5 h, after which crystals were filtered off, washed with cold water and diethylether, and dried under vacuum. Yield: 0.32 mg (57%). ^{1}H NMR (500 MHz, DMSO-d_6, room temperature) (ppm/TMS): δ 2.36 (s, 3H, Ar−C$\underline{H}_3$), 2.43 (s, 3H, 2′-C$\underline{H}_3$), 4.77 (d, 2H, $^3J(^1H,^1H) = 5.5$ Hz, 5′-C$\underline{H}_2$−), 5.42 (t, 1H, $^3J(^1H,^1H) = 5.5$ Hz, 5″-O$\underline{H}$), 7.30−7.45 (m, 4H, −C$_6\underline{H}_4$−), 7.98 (s, 1H, $\underline{H}$6), 9.18 (d, 1H, $^2J(^{15}N,^1H) = 3.4$ Hz, $\underline{H}$4′), 14.06 (s, 1H, $\underline{H}$3′).

8. ^{15}N-Labeled 5′-Triisopropylsilyl Ether of *N*-(Pyridoxylidene)-tolylamine (VII). This synthesis was used to protect the selective ^{15}N-labeling in the imino or in the ring position, depending on the ^{15}N-labeling of the starting material. In 2 mL of abs DMF, 140 mg (0.55 mmol) of ^{15}N-labeled *N*-(pyridoxylidene)tolylamine was dissolved, with stirring under an inert gas atmosphere. Then, 94 mg (1.38 mmol) of imidazole was added. After a few minutes of stirring, 126 mg (0.66 mmol) of triisopropylsilyl chloride was added dropwise. The molar ratio of reactant/chlorosilane/imidazole was 1:1.2:2.5. The solution was stirred under an inert atmosphere for 3 days. The reaction was monitored by TLC (silica, CH_2Cl_2/MeOH 10:0.3). The reaction was stopped by dropping the mixture into 25 mL of 1 M sodium hydrogen carbonate solution. The aqueous phase was extracted two times with 100 mL of dist hexane. The combined organic phases were dried over $NaHCO_3$.

(71) Chang, Y. C.; Graves, D. J. *J. Biol. Chem.* **1985**, *260*, 2709−2714.
(72) Iwanami, M.; Numata, T.; Murakami, M. *Bull. Chem. Soc. Jpn.* **1968**, *41*, 161−165.
(73) Muhlradt, P. F.; Morino, Y.; Snell, E. E. *J. Med. Chem.* **1967**, *10*, 341−344.
(74) Wehrle, B.; Zimmermann, H.; Limbach, H. H. *J. Am. Chem. Soc.* **1988**, *110*, 7014−7024.
(75) Harruff, R. C.; Jenkins, W. T. *Org. Magn. Reson.* **1976**, *8*, 548−557.
(76) Witherup, T. H.; Abbott, E. H. *J. Org. Chem.* **1975**, *40*, 2229−2234.

The solvent was removed, leaving a yellow oil. The crude product was purified by column chromatography (silica, CH_2Cl_2/CH_3OH, 100:1). It was necessary to use HPLC under the same conditions to purify the final product. The products were stored under inert gas at 5 °C. All products were analyzed by mass spectroscopy, and the ^{15}N isotopic enrichment was estimated in the case of the single ring to be >80%, and for the imino-labeled case, it was >90%. Yield: 97 mg (42.5%). 5′-Triisopropylsilyl ether of **VIb** (ring ^{15}N-labeled). ^1H NMR (500 MHz, $CDCl_3$, room temperature) (ppm/TMS): δ 1.05 (m, 21H, Si(CH(CH$_3$))$_3$), 2.38 (s, 3H, Ar−CH$_3$), 2.50 (d, 3H, $^2J(^{15}N,^1H)$ = 3.0 Hz, 2′-CH$_3$), 4.95 (s, 2H, 5′-CH$_2$−), 7.29 (s, 4H, −C$_6$H$_4$−), 7.94 (d, 1H, $^2J(^{15}N,^1H)$ = 10.5 Hz, H6), 9.19 (s, 1H, H4′), 14.07 (s, 1H, H3′). 5′-Triisopropylsilyl ether of **VIc** (imino ^{15}N-labeled). ^1H NMR (500 MHz, CD_2Cl_2, room temperature) (ppm/TMS):δ 1.05 (m, 21H, Si(CH(CH$_3$))$_3$), 2.38 (s, 3H, Ar−CH$_3$), 2.50 (s, 3H, 2′-CH$_3$), 4.95 (s, 2H, 5′-CH$_2$−), 7.29 (s, 4H, −C$_6$H$_4$−), 7.94 (s, 1H, H6), 9.21 (d, 1H, $^2J(^{15}N,^1H)$ = 2.9 Hz, H4′), 14.03 (s, 1H, H3′).

9. ^{15}N-Labeled (Ring and Doubly) *N*-(Pyridoxylidene)methylamine (VIIIa,b). To 90 mg (0.53 mmol) of ^{15}N-labeled pyridoxine (**V**) dissolved in 10 mL of water was added a freshly prepared, 20 mL aqueous solution with manganese dioxide (prepared from 0.3 g of potassium permanganate, 0.4 g of sodium bisulfite and 0.4 mL of 50% sulfuric acid with stirring for 30 min). After standing overnight, the pH was adjusted with 1 M $NaHCO_3$ solution to 7.78. To the reaction mixture was added dropwise a solution of 50 mg (0.75 mmol) of methylamine hydrochloride or (95%) ^{15}N-labeled methylamine hydrochloride. The pH was readjusted to 7.8. After stirring for several hours at room temperature, the product was extracted with dichloromethane. The combined organic phases were dried over $NaHCO_3$. The solvent was removed, and the product was dried under vacuum overnight. The yellow crude product was dissolved in CH_2Cl_2 and purified by column chromatography (cellulose, CH_2Cl_2) monitored by ^1H NMR in the liquid state. Thirty milligrams (0.22 mmol) of doubly ^{15}N-labeled **VIIIb** was obtained and analyzed by low-temperature, liquid-state ^1H NMR. Yield: 0.22 mg (42%). ^1H NMR (500.13 MHz, CD_2Cl_2, 230 K) (ppm/TMS): δ 2.39 (s, 3H, 2′-CH$_3$), 3.14 (s, 1H, H5″ (−OH)), 3.52 (s, 3H, N−CH$_3$), 4.69 (s, 2H, 5′-CH$_2$−), 7.63 (d, 1H, H6, $^2J(^{15}N,^1H)$ = 10.45 Hz), 8.82 (s, 1H, H4′), 14.60 (d, 1H, $^1J(^{15}N,^1H)$ = 5.61 Hz, H3′). ^{15}N {^1H} NMR (50.61 MHz, CD_2Cl_2, 190 K) (ppm/$^{15}NH_4Cl$): δ 171 ppm (s, N2,^{15}N−CH$_3$), 166 ppm (s, N1 ring).

10. ^{15}N-Labeled (Imino) *N*-(Pyridoxylidene)methylamine (VIIIb). An aqueous solution of 300 mg (1.47 mmol) of pyridoxal hydrochloride was neutralized with $NaHCO_3$; 100 mg (1.47 mmol) of (95% ^{15}N) methylamine hydrochloride was added, and the reaction mixture was adjusted with 1 M $NaHCO_3$ to pH 7. After stirring for several hours at room temperature, the product was extracted with dichloromethane. The solvent was removed, and a yellow product, ^{15}N-(pyridoxylidene)-methylamine, was obtained in a yield of 193 mg (73%). The product was analyzed by low-temperature liquid-state ^1H NMR and mass spectrometry; ^{15}N isotopic enrichment was estimated to be >88%. Yield: 193 mg (73.0%). Mp 145−146 °C (146−151 °C[63,64]). ^1H NMR (500.13 MHz, CD_2Cl_2, 190 K) (ppm/TMS): δ 2.24 (s, 3H, 2′-CH$_3$), 3.47 (s, 3H, N−CH$_3$), 4.53 (s, 2H, 5′-CH$_2$−), 6.51 (s, 1H, H5″ (−OH)), 7.71 (s, 1H, H6), 8.78 (s, 1H, H4′), 14.85 (d, 1H, $^1J(^{15}N,^1H)$ = 10.3 Hz, H3′). ^{15}N {^1H} NMR (50.61 MHz, CD_2Cl_2, 300 K) (ppm/$^{15}NH_4Cl$): δ 252.36 (s,^{15}N−CH$_3$).

11. ^{15}N-Labeled *p*-Toluidine (IX). This was prepared from *p*-toluyl chloride and $^{15}NH_4Cl$ followed by treatment of the ^{15}N-labeled *p*-toluamide obtained with sodium hypobromite solution. The synthesis of ^{15}N-labeled *p*-toluidine was described previously.[59,60] The product was checked by mass spectrometry, and the ^{15}N isotopic enrichment was estimated to be 96%.

12. ^{15}N-Labeled (Imino) Pyridoxamine (PM) (X). This was prepared from 5 g (24.5 mmol) of pyridoxal hydrochloride and 1.0 g (14.2 mmol) of ^{15}N-enriched hydroxylamine hydrochloride, which reacts with sodium acetate to give the oxime. The oxime was hydrogenated with platinic oxide in ethanolic hydrochloric acid to the ^{15}N-labeled product. The product reacted positively with ninhydrin (TLC, 1% in acetone). Detailed procedures are described in refs 67−70. Yield: 200 mg (9%, based on used $^{15}NH_2OH{\cdot}HCl$). ^1H NMR (500.13 MHz, D_2O, 190 K) (ppm/TMS): δ 2.48 (s, 3H, 2′-CH$_3$), 4.31 (s, 2H, 4′-CH$_2$−$^{15}NH_3^+$), 4.71 (s, 2H, 5′-CH$_2$−), 7.61 (s, 1H, H6).

13. ^{15}N-Labeled Pyridoxal (PL) (XI). An amount of 180 mg (0.99 mmol) of the ^{15}N-labeled **VIIIb** was stirred for 1 h in 1 M hydrochloric acid. The crude product was purified two times by column chromatography (silica, CH_2Cl_2/CH_3OH, 100:12). After the purification, the pyridoxal hydrochloride was neutralized with sodium hydrogen carbonate and was then lyophilized. The product was analyzed by analytical HPLC (Luna C8(2) column; eluent acetonitrile/water/trifluoroacetic acid, 95/5/0.1%). Yield: 70 mg (41%). (Purity according to NMR <70%.) ^1H NMR (500.13 MHz, D_2O, 190 K, PL in cyclic hemiacetal form[63]) (ppm/TMS): δ 2.46 (s, 3H, 2′-CH$_3$), 5.14 (s, 1H, H5′a), 5.18 (d, $^4J(^1H,^1H)$ = 1.9 Hz, 1H, H5′b), 6.58 (d, $^4J(^1H,^1H)$ = 1.9 Hz, 1H, H4′), 7.57 (d, $^2J(^{15}N,^1H)$ = 3.8 Hz, 1H, H6).

14. ^{15}N-Labeled Pyridoxal-5′-phosphate (PLP) (XII). Under an inert gas stream, 6.50 g of conc phosphoric acid, H_3PO_4, and 5.00 g of phosphorus pentoxide, P_2O_5, were mixed. To the chilled mixture was added 1.0 g (3.9 mmol) of **VIa**. The viscous mixture was mixed thoroughly and heated for 9 h at 40 °C under a constant inert gas stream. The reaction mixture was then chilled on ice, 5 mL of 0.1 M hydrochloric acid was added slowly, and the solution was heated for 10 min at 60 °C, followed by standing overnight. The reaction mixture was diluted with water and applied to a strong cationic exchanger (Amberlite IR-120; 0.3−1.2 mm (15−50 mesh ASTM)) and eluted with water. The product was isolated by using a flow rate of 1 drop/s. All fractions were checked by TCL (silica gel, CH_2Cl_2/CH_3OH, 2:3). The combined fractions were lyophilized, and a yellow powder was obtained. The product was analyzed by mass spectrometry, and the ^{15}N isotopic enrichment was estimated to be >80%. Yield: 0.2 g (21%). ^1H NMR (500 MHz, DMSO-d_6, room temperature) (ppm/TMS): δ 2.43 (s, 3H, 2′-CH$_3$), 5.19 (d, $^3J(^{31}P,^1H)$ = 6.8 Hz, 2H, 5′-CH$_2$−), 8.12 (d, $^2J(^{15}N,^1H)$ = 10.8 Hz, 1H, H6), 10.3 (s, 1H, H4′). ^{31}P {^1H} NMR (202.46 MHz, D_2O, room temperature) (ppm/85% H_3PO_4): δ 2.7 (s, 1P, −PO$_3^{2-}$).

D. Preparation of NMR Samples. 1. Preparation of Polycrystalline Powders 1a−1j. Polycrystalline powders of the ^{15}N-labeled *N*-(pyridoxylidene)tolylamine (**1b**) and their 1:1 acid-base complexes **1b**−^{15}N−3,5-dichlorobenzoic acid (**1c**), **1b**−^{15}N−3-nitro-4-chlorobenzoic acid (**1d**), **1b**−^{15}N−4-nitrobenzoic acid (**1e**), **1b**−^{15}N−2-nitrobenzoic acid (**1f**), **1b**−^{15}N−3,5-dinitrobenzoic acid (**1g**), **1b**−^{15}N−3,5-dinitro-4-methylbenzoic acid (**1h**), **1b**−^{15}N−hydrochloric acid (**1i**), and **1b**−^{15}N−trichloroacetic acid (**1j**) were prepared as follows. Solutions of the purified compounds in dichloromethane were evaporated, washed with diethylether, and dried under high vacuum overnight. The compounds were deuterated by repeated distillation from methanol-d_1, leading to **1b**-*d*, **1g**-*d*, and **1j**-*d*, which were dried under high vacuum overnight. Complex **1i**-*d* was prepared from DCl solution in D_2O and lyophilized. The extents of deuteration, reported in Table 2, were estimated by integration from ^1H NMR liquid state spectra.

2. Preparation of Polycrystalline Powders 2a−2e. Polycrystalline powders of the ^{15}N-labeled *N*-(pyridoxylidene)methylamine (**2a**) and their 1:1 acid-base complexes **2a**−^{15}N−4-chlorobenzoic acid (**2b**), **2a**−^{15}N−4-nitrobenzoic acid (**2c**), and **2a**−^{15}N−3,5-dinitrobenzoic acid (**2d**) were prepared as follows. Solutions of the purified compounds in methanol were evaporated and dried. In the case of **2a**−^{15}N−4-tolylsulfonic acid (**2e**), dioxane was used instead, in order to avoid decomposition, and was removed under reduced pressure at 40 °C. Unlabeled samples of **2a** to **2e** for solid state ^1H and ^{15}N NMR measurements at natural abundance were prepared in a similar way. The stability of **2a** in the complexes was analyzed by ^1H NMR in the liquid state. Deuteration of the ^{15}N-imino-labeled (**2a**) and the **2a**−4-nitrobenzoic adduct (**2c**) was performed by repeated distillation of

Table 1. NMR Parameters for the Aldenamine and Aldimine Schiff Bases and their 1:1 Acid-Base Complexes with Benzoic Acid Derivatives

acid–base complexes		pK_a[a] –OH1	$\delta(^1H)$ O1H1N1 ±1.0 /ppm	$\delta(^{15}N)$[b] O1H1N1 ±1.0 /ppm	$\delta(^1H)$ O2H2N2 /ppm	$\delta(^{15}N)$[c] O2H2N2 ±1.0 /ppm	$^1\Delta N2(D)$[d] N2 ±2.0 /ppm
aldenamine Schiff base:							
protected **1b**	**1a**			282.5(0)	13.6	254.6(−21.4)	
1b (free base)	**1b**			261.8(−20.7)	14.2	253.6(−22.4)	3.0
1b + 3,5-dichloro b. a.	**1c**	3.14	18.2	222.3(−60.2)	14.7	249.6(−26.4)	
1b + 3-nitro-4-chloro b. a.	**1d**	3.66	18.8	210.9(−71.6)	14.8	250.1(−25.9)	
1b + 4-nitro b. a.	**1e**	3.44	20.2	205.5(−77.0)	14.2	265.0(−11.0)	
1b + 2-nitro b. a.	**1f**	2.17	18.7	187.4(−95.1)	14.0	261.0(−15.0)	
1b + 3,5-dinitro b. a.	**1g**	2.82	18.3	177.9(−104.6)	15.5	246.8(−29.3)	
1b + 3,5-dinitro-4-methyl b. a.	**1h**	2.97	18.2	177.6(−104.9)	14.8	252.7(−23.3)	
1b + hydrochloric acid	**1i**	−7.0	15.8	170.3(−112.2)	15.8	244.4(−31.6)	
1b + trichloroacetic acid	**1j**	0.66	15.8	166.3(−116.2)	16.8	238.0(−38.0)	
aldimine Schiff base:							
2a (free base)	**2a**			268.5(−14.0)[f]	13.6[e]	261.2(−18.8)	2.9
2a + 4-chloro b. a.	**2b**	3.99	19.0	192.4(−90.1)[g]	14.3	147.8(−132.2)	
2a + 4-nitro b. a.	**2c**	3.44	18.4	182.3(−100.2)[f]	14.1	144.3(−135.7)	−3.4
2a + 3,5-dinitro b. a.	**2d**	2.82	17.2	181.1(−101.4)[g]	14.4	150.0(−130.0)	
2a + 4-tolylsulfonic acid	**2e**	−6.65	15.1	163.8(−118.7)[g]	14.0	138.6(−141.4)	
PLP and analogues:							
pyridoxal-5′-phosphate	PLP			170.2(−112.3)			
pyridoxine	PN			249.5(−33.0)			
pyridoxine hydrochloride	PN·HCl			158.3(−124.2)			
pyridoxal	PL			164.8(−117.7)			
pyridoxamine dihydrochloride	PM·2HCl			170.6(−111.9)		10.9[h]	
pyridoxamine	PM					−4.3[i]	

[a] pK_a values of the acid proton H1 involved in the intermolecular O1H1N1 hydrogen bond, obtained from refs 83−86. [b] Values of δ(O1H1N1) for the pyridine nitrogen in brackets are with respect to solid **1a**, resonating at 282.5 ppm. [c] With respect to the methoxy-protected Schiff base,[20] resonating at 276 and 280 ppm for the **1** and **2**, respectively.[94,95] [d] The secondary isotope effect $^1\Delta N2(D)$ is defined as $^1\Delta N(D) = \delta(ODN) - \delta(OHN)$.[40] [e] The other signal was assumed to be due to the small geometrical changes in the centrosymmetric dimer.[46] [f] From the doubly ^{15}N-labeled aldimine Schiff base. [g] Obtained from spectra at natural abundance. [h] Ammonium group $-NH_3^+Cl^-$. [i] The amine group from ^{15}N-imino-labeled PM. All ^1H and ^{15}N chemical shifts are with respect to external solid TSP and $^{15}NH_4Cl$, respectively.

Table 2. Chemical Shielding Parameters of Hydrogen-Bonded Acid-Base Complexes

solid state 1:1 acid–base complexes		% D	δ_{xx}[b] ±1 /ppm	δ_{yy}[b] ±1 /ppm	δ_{zz}[b] ±1 /ppm	δ_{iso}^{calcd}[c] ±3 /ppm	δ_{iso}^{exptl}[a] ±1.0 /ppm	$^1\Delta N1(D)$[d] ±2.0 /ppm	D_{DN}[e] ±75 /Hz	r_{DN}[f] ±0.08 /Å
aldenamine Schiff base	**1b**	0	343	488	−37	265	261.8			
1b + 3,5-dinitro b. a.	**1g**	0	301	253	−9	182	177.9			
1b + hydrochloric acid	**1i**	0	284	217	−11	163	170.3			
1b + trichloroacetic acid	**1j**	0	286	206	0	164	166.3			
deuterated **1b**										
1b-*d* + 3,5-dinitro b. a.	**1g**-*d*	60	305	233	−13	175	172.9	−5.0	1286	1.13[g]
1b-*d* + hydrochloric acid	**1i**-*d*	100	284	217	−11	163	168.5	−1.8	1349	1.11
1b-*d* + trichloroacetic acid	**1j**-*d*	100	286	206	0	164	165.5	−0.8	1481	1.08[h]

[a] δ_{iso}^{exptl}: ^{15}N isotropic chemical shift from ^{15}N CP MAS spectra and referenced to external solid $^{15}NH_4Cl$. [b] δ_{xx}, δ_{yy}, δ_{zz}: the components of the CSA tensor. [c] $\delta_{iso}^{calcd} = 1/3(\delta_{xx} + \delta_{yy} + \delta_{zz})$. [d] $^1\Delta N1(D)$: secondary isotope effect is defined as $^1\Delta N1(D) = \delta(ODN) - \delta(OHN)$. [e] D_{DN}: dipolar coupling constants. [f] r_{DN}: cubic average distances, N···D, obtained by line-shape analysis. Euler angles in the coordinate system of the CSA tensor were set to 0 and 90°. [g] With a predicted r_{OH} distance of 1.45 Å. [h] With a predicted r_{OH} distance of 1.60 Å. For further details on the theory of the dipolar heteronuclear coupling, see Supporting Information.

methanol-d_1 from the sample at room temperature, leading to **2a**-*d* and **2c**-*d*, which were dried under high vacuum overnight. The percent deuteration in both compounds was >50%, as checked by integration of ^1H NMR liquid state spectra.

3. Preparation of PLP and PLP Analogues. The syntheses of the ^{15}N-labeled PM, PLP, and PN in the neutral and hydrochloride form are described in the preceding sections. Pyridoxal hydrochloride (PL·HCl) from Aldrich was neutralized with 1 M $NaHCO_3$ to PL and then lyophilized. Pyridoxamine hydrochloride (PM·HCl) from Aldrich was used without further purification.

Theoretical Section

Geometric and NMR Hydrogen Bond Correlations. In previous work, it has been shown that the valence bond orders defined by Pauling[77] are useful for describing geometric correlations of hydrogen bonds of the general type A−H···B.[78−81] The bond valences p_i of the A−H and of the H···B bonds are defined as described in the following, and in the valence bond framework, it is assumed that the total bond order to hydrogen is unity, for example, $p_1 + p_2 = 1$.[82]

$$p_1 = \exp\{-(r_1 - r_1^{o})/b_1\} \text{ and } p_2 = \exp\{-(r_2 - r_2^{o})/b_2\} \quad (1)$$

Here, $r_1 = r_{AH}$ represents the A···H distance, $r_2 = r_{HB}$ is the

(77) Pauling, L. *J. Am. Chem. Soc.* **1947**, *69*, 542−553.
(78) Steiner, T. *Angew. Chem., Int. Ed.* **2002**, *41*, 48−76.
(79) Steiner, T.; Majerz, I.; Wilson, C. C. *Angew. Chem., Int. Ed.* **2001**, *40*, 2651−2654.
(80) Steiner, T.; Wilson, C. C.; Majerz, I. *Chem. Commun.* **2000**, 1231−1232.
(81) Steiner, Th. *J. Phys. Chem. A* **1998**, *102*, 7041−7052.
(82) Brown, I. D. *Acta Crystallogr., Sect. B* **1992**, *48*, 553−572.

H···B distance, and p_1 and p_2 are the corresponding valence bond orders of the diatomic units. The parameters r_1^o and r_2^o are the equilibrium distances in the hypothetical free diatomic units AH and HB, while b_1 and b_2 are the parameters describing the decays of the bond order when the bond is stretched. Therefore, it follows that r_1 and r_2 depend on each other. For OHN hydrogen bonds, Steiner[81] proposed the parameter set $r_{OH}^o = 0.942$, $r_{HN}^o = 0.992$, $b_{OH} = 0.371$, and $b_{HN} = 0.385$ Å. Recently, it was assumed that these equations are only valid for equilibrium geometries, as zero-point vibrations were not taken into account.[39,40] In order to take the latter into account, the following empirical bond order equations for the equilibrium bond orders were proposed[39,40]

$$p_1^H = p_1 - c^H(p_1p_2)^f(p_1 - p_2) - d^H(p_1p_2)^g = \exp\{-(r_1^H - r_1^o)/b_1\}$$

$$p_2^H = p_2 + c^H(p_1p_2)^f(p_1 - p_2) - d^H(p_1p_2)^g = \exp\{-(r_2^H - r_2^o)/b_2\} \quad (2)$$

The parameters $c^H = 360$, $d^H = 0.7$, and $f = 5$, $g = 2$ were used and have been adapted empirically to the case of OHN hydrogen bonds to heterocyclic bases.[40] Expressing the correlation in terms of normal coordinates, defined as $q_1 = 1/2(r_1 - r_2)$ and $q_2 = r_1 + r_2$, is useful. For a linear hydrogen bond, q_1 represents the deviation of the proton distance from the hydrogen bond center, while q_2 represents the distance between the heavy atoms A and B, as indicated in Scheme 6. Note that the correlation is independent of the hydrogen bond angle. Herein, A−H···B corresponds to the intra- and intermolecular OHN hydrogen bond in the Schiff base model complexes (Scheme 3); A is oxygen of the carboxylic acid or the phenolic group, and B is the ring or imino nitrogen of the Schiff bases. A typical correlation curve[40] of q_2 versus q_1 will be presented later (solid line in Figure 3a); it shows that, when the proton is transferred from A to B, a hydrogen bond contraction occurs that is maximal when the proton is located approximately in the hydrogen bond center. In order to visualize the quantum effects, a typical corrected[40] q_2 versus q_1 curve is also presented later (dashed line in Figure 3a). Throughout this paper, the corrected bond valences are used in order to describe experimental data because the equilibrium bond valences can be used only as an approximation.

The bond orders are additionally useful for deriving correlations between NMR parameters and hydrogen bond geometries.[34−40] The following relations were proposed for the chemical shifts of OHN hydrogen bonds.

$$\delta(\mathrm{OH\underline{N}}) = \delta(\underline{\mathrm{N}})^o p_{OH}^H + \delta(\mathrm{H\underline{N}})^o p_{HN}^H + 4\delta(\mathrm{OH\underline{N}})^* p_{OH}^H p_{HN}^H \quad (3)$$

$$\delta(\mathrm{O\underline{H}N}) = \delta(\mathrm{O\underline{H}})^o p_{OH}^H + \delta(\underline{\mathrm{H}}\mathrm{N})^o p_{HN}^H + 4\delta(\mathrm{O\underline{H}N})^* p_{OH}^H p_{HN}^H \quad (4)$$

The pK_a values associated with the acidic proton in the acid-base complexes can be related to q_1^H.[35,41]

$$\mathrm{p}K_a = A - Bq_1^H \quad (5)$$

Here, $\delta(\underline{\mathrm{N}})^o$, $\delta(\mathrm{H\underline{N}})^o$, $\delta(\mathrm{O\underline{H}})^o$, and $\delta(\underline{\mathrm{H}}\mathrm{N})^o$ represent the chemical shifts of the hypothetical free molecular units into which the OHN hydrogen bond can formally dissociate. The parameters $\delta(\mathrm{OH\underline{N}})^*$ and $\delta(\mathrm{O\underline{H}N})^*$ are the "excess" terms that describe the deviation of the quasisymmetric hydrogen bond from the average of the hypothetical limiting molecular units. These parameters were obtained by fitting the calculated data points to the experimental ones, as discussed later in this paper.

Scheme 6. (a) Parameters Characterizing Geometry of the Hydrogen Bond: Distances r_{AH}, r_{BH} and the Angle α. (b) Definition of $q_1 = 1/2(r_{AH} - r_{HB})$ and $q_2 = r_{AH} + r_{HB}$ as the Divergence of the Proton from the Center of the Bond and the Heavy Atom Distance, Respectively

Results

The results of the solid state ^{1}H and ^{15}N NMR experiments are depicted in Figures 1 and 2 and in Figures S1−S5 of the Supporting Information. All parameters obtained are gathered in Tables 1 and 2.

A. The Aldenamine Schiff Bases and Their Acid−Base Adducts. The ^{1}H MAS NMR solid state spectra of **1a**−**1j** were observed using a fast-spinning speed of 24 kHz. Since fast spinning removes homonuclear dipolar coupling, to a large extent, we were able to observe the signals of the hydrogen-bonded protons of the intra- and intermolecular OHN hydrogen bonds depicted on the left side of Figure 1. When the acidity of the carboxylic acid[83−86] is increased, the ^{1}H signal of the intermolecular O1H1N1 hydrogen bond (labeled as H1 in Figure 1) is shifted from 18.2 ppm to a maximum of 20.2 ppm and then back to 15.8 ppm. A similar behavior was observed previously for 2,4,6-trimethylpyridine-acid complexes in the organic solid state.[35] At the same time, the proton of the intramolecular O2H2N2 hydrogen bond (labeled as H2 in Figure 1) is slightly shifted from 14 to 16 ppm. In the **1b**−hydrochloric acid adduct (**1i**), only one signal at 15.8 ppm was detected for both hydrogen-bonded protons.

The ^{15}N spectra of compounds **1a**−**1j**, singly ^{15}N-labeled in the ring position, are presented in the center column of Figure 1. The signals shifted monotonically to the high field with the increasing acidity of the proton donor. Compound **1a** resonates at a lower field than **1b** because of intermolecular O1H1N1 hydrogen bonds between the hydroxyl groups of **1b** and the pyridine ring.[46] These measurements helped to assign the ^{15}N signals of the intramolecular O2H2N2 hydrogen bond (imino nitrogen N2) in the doubly ^{15}N-labeled compounds, depicted in the right column of Figure 1.

In the corresponding deuterated compounds, **1g**-*d*, **1i**-*d*, and **1j**-*d* (see Figure S1 of the Supporting Information), high-field shifts of the ring nitrogen signals were observed, indicating the presence of secondary H/D isotope effects, $^1\Delta\mathrm{N(D)} = \delta(\mathrm{OD\underline{N}}) - \delta(\mathrm{OH\underline{N}})$, on the ^{15}N chemical shifts and hence changes in the intermolecular O1H1N1 hydrogen bond geometries.[40]

The chemical shifts of the imino nitrogen N2 are fairly constant from **1a** to **1d**. Then, a small low-field shift occurs

(83) Polansk, J.; Bak, A. *J. Chem. Inf. Comput. Sci.* **2003**, *43*, 2081−2092.
(84) Kortüm, G.; Vogel, N.; Andrussow, K. *Dissociation Constants of Organic Acids in Aqueous Soluions*; Butterworth: London, 1961.
(85) French, D. C.; Crumrine, D. S. *J. Org. Chem.* **1990**, *55*, 5494−5496.
(86) Crumrine, D. S.; Shankweiler, J. M.; Hoffman, R. V. *J. Org. Chem.* **1986**, *51*, 5013−5015.

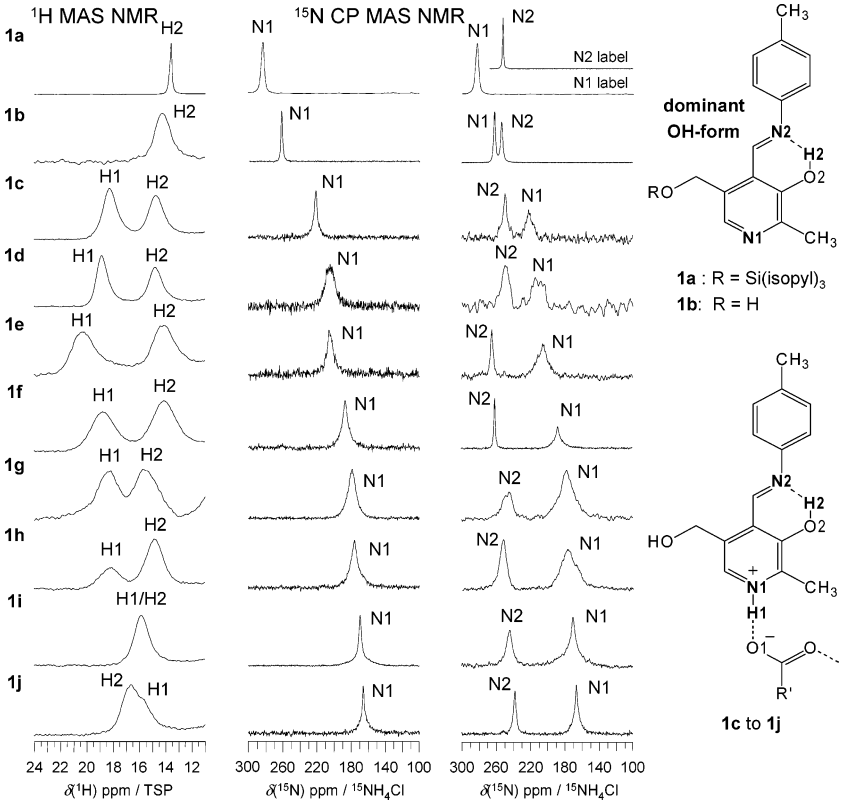

Figure 1. Solid state spectra of the aldenamine Schiff bases **1b** and their 1:1 acid-base complexes with benzoic acid derivatives **1a**−**1j**. From the left are shown ^{1}H MAS ECHO NMR spectra, 600 MHz, 24 kHz; ^{15}N {^{1}H} CP MAS spectra, 30.41 MHz, 6 kHz, ^{15}N ring-labeled **1a**−**1j**; ^{15}N {^{1}H} CP MAS spectra, 30.41 MHz, 6 kHz; ^{15}N doubly labeled **1a**−**1j**.

(**1e**), followed again by small upfield shifts (**1f**−**1j**). For the deuterated compound **1b**-*d*, a 3 ppm shift to a lower field of the imino nitrogen signal (not shown) was observed, indicating a secondary H/D isotope effect, $^{1}\Delta$N2(D), on the intramolecular O2H2N2 hydrogen bond geometry.

In order to estimate the hydrogen-nitrogen distances in the intermolecular O1H1N1 hydrogen bond, we measured the ^{1}H-decoupled ^{15}N CP NMR spectra of static deuterated powdered compounds **1g**-*d*, **1i**-*d*, and **1j**-*d* at 30.41 MHz (see Figure S1 of the Supporting Information). They contain information about the chemical shift anisotropy of the pyridine nitrogen and the dipolar ^{2}H−^{15}N coupling. The spectra were analyzed as described previously for 2,4,6-trimethylpyridine-acid complexes.[35] As in this reference, the spectra were simulated by assuming that the N···D axis coincides with the NC4 axis, that is, that it is parallel to δ_{yy}. This assumption has been used and justified using ab initio methods by Solum et al.[87] in the case of pyridine and pyridinium salts. Thus, only the values of the dipolar coupling constants D^{DN} were varied but not the Euler angles relating the chemical shielding and the dipolar DN coupling tensors.

The parameters of the chemical shielding tensor and the cubic-averaged ^{2}H−^{15}N distances, r_{DN}, obtained are listed in Table 2. Additional details on the theory of dipolar ^{15}N solid state NMR[88−93] are given in the Supporting Information.

B. The Aldimine Schiff Bases and Their Acid−Base Adducts. A collection of typical NMR spectra of the polycrystalline aldimine Schiff bases **2a** and their 1:1 acid-base complexes with benzoic acid derivatives **2a**−**2e** are depicted in Figure 2. The ^{1}H MAS spectra of **2a**−**2e** are in the left column, the ^{15}N CP MAS NMR spectra of the ^{15}N selectively imino-labeled adducts are in the center column, and the corresponding spectra at natural ^{15}N abundance are in the right column, which helped to assign the ^{15}N signals. We assign the proton signal of aldimine Schiff base **2a** at 13.6 ppm to the intramolecular O2H2N2 hydrogen bond. Another low-field proton signal of **2a** at 15 ppm was observed, which was difficult to assign. According to the X-ray crystallographic structure, the aldimine Schiff base **2a** forms cyclic centrosymmetric dimers in the solid state,[46] containing two intermolecular O1H1N1 hydrogen bonds between the side-chain hydroxyl groups and the pyridine rings. As a consequence, the low-field proton signal can be assigned to small geometrical changes in the intramolecular O1H2N1 hydrogen bonds, which result in two different proton signals. On the other hand, the possibility that this signal derives from the intermolecular O1H1N1 hydrogen bond, where the side-chain hydroxyl group is involved, is less possible since the signal is located at too low field for such a group.[20] In the adduct **2b** with *p*-chlorobenzoic acid, the proton in the intermolecular O1H1N1 hydrogen bond was observed at 19.0 ppm

(87) Solum, M. S.; Altmann, K. L.; Strohmeier, M.; Berges, D. A.; Zhang, Y.; Facelli, J. C.; Pugmire, R. J.; Grant, D. M. *J. Am. Chem. Soc.* **1997**, *119*, 9804−9809.
(88) Mehring M. *NMR Basic Principles and Progress 11, High Resolution NMR in Solids*; Springer: Berlin, Germany, 1978.
(89) Gullion, T.; Schaefer J. In *Advances in Magnetic Resonance*; Warren, W. S., Ed.; Academic Press: San Diego, CA, 1989; Vol. 13, p 57.
(90) Hoelger, C.-G.; Limbach, H. H. *J. Phys. Chem.* **1994**, *98*, 11803−11810.
(91) Bork, V.; Gullion, T.; Hing, A.; Schaefer, J. *J. Magn. Reson.* **1990**, *88*, 523−532.
(92) Hughes, E.; Gullion, T.; Goldbourt, A.; Vega, S.; Vega, A. J. *J. Magn. Reson.* **2002**, *156*, 230−241.
(93) Gullion, T. *J. Magn. Reson.* **2000**, *146*, 220−222.

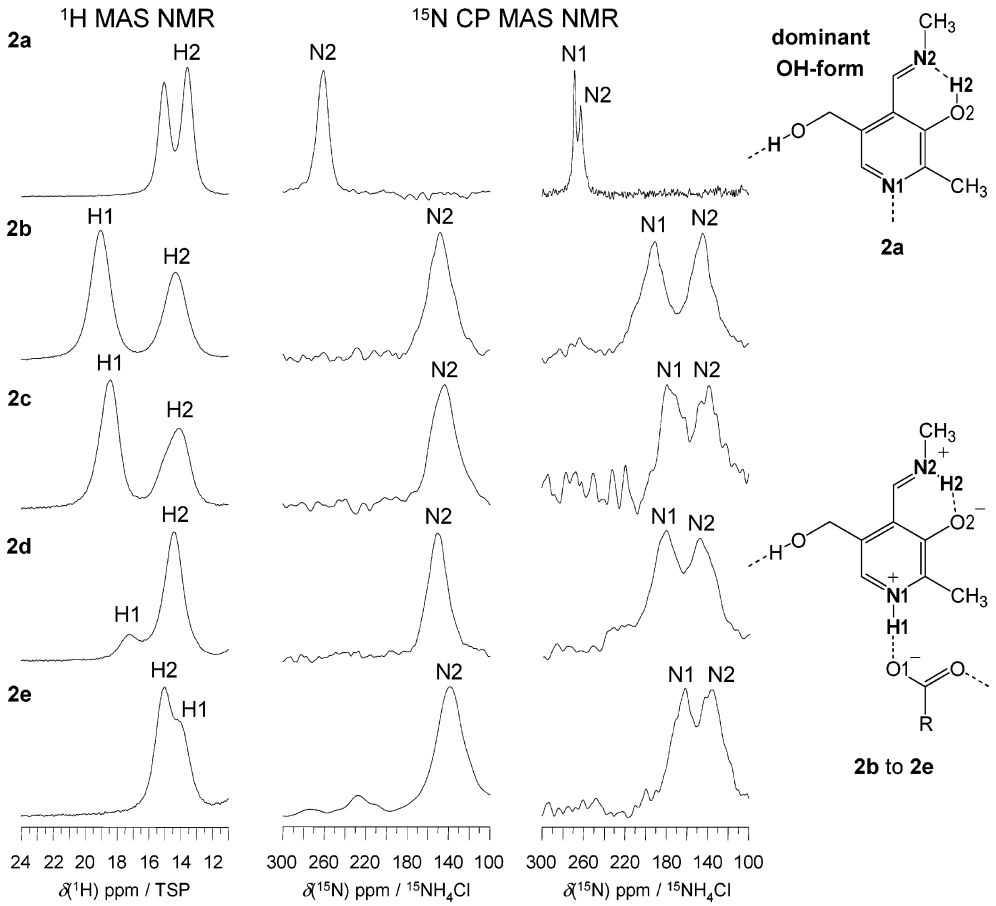

Figure 2. Solid state spectra of the aldimine Schiff bases **2a** and their 1:1 acid-base complexes with benzoic acid derivatives **2b**−**2e**. From the left are shown ^{1}H MAS ECHO NMR spectra, 600 MHz, 24 kHz; ^{15}N {^{1}H} CP MAS spectra, 30.41 MHz, 6 kHz, ^{15}N-imino-labeled **2a**−**2e**; ^{15}N {^{1}H} CP MAS spectra, 30.41 MHz, 6 kHz, in natural abundance; **2a** and **2c** are ^{15}N doubly labeled.

and was high field shifted to 14.1 ppm in **2e** when the acidity of the acid increased.

In **2a**, both the pyridine nitrogen signal N1 and the Schiff base nitrogen signal N2 appear at a low field but abruptly shifted to a high field, indicating protonation of both nitrogens when the adducts were formed. Deuteration leads to a low-field shift of 2.9 ppm of the N2 signal in **2a**-*d* but leads to a high-field shift of −3.4 ppm in the adduct **2c**-*d* with 4-nitrobenzoic. The ^{15}N spectra of the deuterated compounds are given in Figure S2 in the Supporting Information.

C. The Cofactors PLP and Their Analogues. Finally, we measured the ^{15}N CP MAS NMR spectra of ^{15}N-labeled PLP, ^{15}N-labeled PN, ^{15}N-labeled PN·HCl, ^{15}N-labeled PM, as well as PL and PN·HCl at natural abundance. These spectra are given in Figures S3−S5 in the Supporting Information. The ^{15}N isotropic chemical shifts are collected in Table 1.

Discussion

We have carried out solid state ^{1}H and ^{15}N NMR experiments on polycrystalline hydrogen-bonded, 1:1 complexes of Schiff bases of the cofactor PLP with carboxylic acids, depicted in Scheme 4. These complexes were designed to mimic the cofactor in the active sites of a variety of enzymes. In particular, we were interested in if and how the intermolecular O1H1N1 hydrogen bond and the intramolecular O2H2N2 hydrogen bond interact which each other. In this section, we first correlate the ^{1}H and ^{15}N solid state NMR parameters with the hydrogen bond geometries, and then, we discuss the crystallographic structures available for the compounds studied here by NMR. Finally, we discuss potential biological implications arising from these results.

A. Hydrogen Bond Distances in PLP and Its Derivatives. Since it is difficult to obtain proton positions using X-ray diffraction, in this section, we discuss ways to obtain this information from the ^{15}N and ^{1}H NMR chemical shifts of PLP and its derivatives.

1. HN Distance−^{15}N Chemical Shift Correlation for the Intermolecular O2H2N2 Hydrogen Bond. We start with a discussion of the geometric correlation for OHN hydrogen bonds obtained from low-temperature neutron crystallographic data reported by Steiner[78−81] and Limbach et al.,[40] depicted in Figure 3a. The solid line represents the correlation between the hydrogen bond coordinates $q_2 = r_{OH} + r_{HN}$ and $q_1 = 1/2(r_{OH} - r_{HN})$, which refer to the equilibrium geometries where zero-point vibrations are not taken into account. According to eq 1, the correlation line depends only on the values of r_1^o and r_2^o, on the equilibrium distances in the hypothetical free diatomic units AH and HB, and on the values of b_1 and b_2, the valence bond decay parameters. In the dashed line of Figure 3a, an empirical correction for zero-point motions according to eq 2 is included,[40] which reproduces the experimental neutron data well, as shown in Figure 3a.

The solid state, dipolar NMR studies on the polycrystalline aldenamine Schiff base-acid complexes **1g**-*d*, **1i**-*d*, and **1j**-*d* allowed the inverse cubic-averaged N···D distances to be

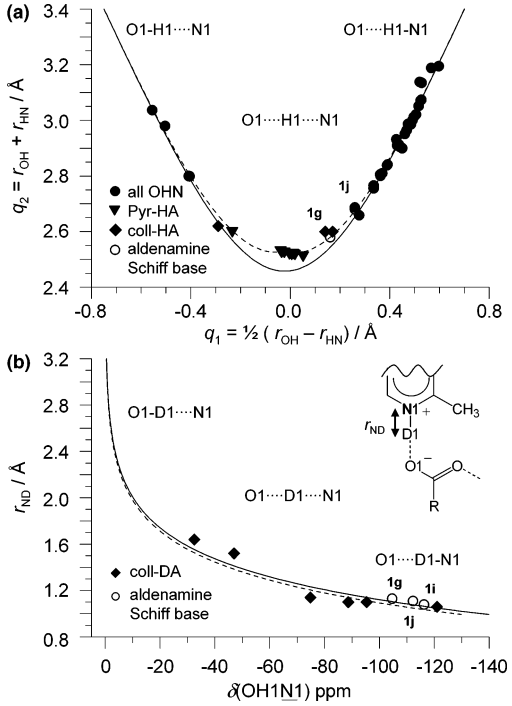

Figure 3. Geometric OHN hydrogen bond correlations. (a) q_2 versus q_1. Equilibrium (solid line) and corrected (dashed line) correlation curves calculated according to ref 40. The circles refer to neutron diffraction geometries.[81] The triangles represent the recently published neutron diffraction data.[78−80] The diamonds correspond to crystalline 2,4,6-trimethylpyridine-acid complexes.[35] The open circles correspond to crystalline aldenamine Schiff base-acid complexes. (b) DN distance versus ^{15}N chemical shift correlation. The diamonds represents the r_{HN} distances for 2,4,6-trimethylpyridine−DA complexes from dipolar, solid state NMR,[35] with respect to the frozen bulk 2,4,6-trimethylpyridine. The dashed line corresponds to the latter complexes by using $\delta(\underline{H}N)^o = -130$.[35,40] The open circles correspond to crystalline aldenamine Schiff base−acid complexes, with respect to solid **1a**, resonating at 282.5 ppm. The solid line corresponds to the latter complexes by using $\delta(\underline{H}N)^o = -140$. For the calculation of the curves, see text.

estimated (cf. Table 2). The corresponding distances r_{OD} of **1g**-*d* and of **1j**-*d* were then varied such that the resulting hydrogen bond coordinates $q_2^D = r_{OD} + r_{DN}$ and $q_1^D = 1/2(r_{OD} - r_{DN})$ of **1g**-*d* and of **1j**-*d* fitted the dashed curve in Figure 3a. The results indicate that the proton is slightly shifted beyond the hydrogen bond center toward the nitrogen.

In Figure 3b, the cubic average r_{DN} distances of pyridine derivatives hydrogen bonded to acids are plotted as a function of their intrinsic ^{15}N chemical shifts. We chose **1a** as a reference for **1g**-*d*, **1i**-*d*, and **1j**-*d* since it is not involved in an intermolecular O1H1N1 hydrogen bond and resonates at 282.5 ppm. The graph also includes the corresponding distances r_{DN} for the polycrystalline 2,4,6-trimethylpyridine-acid complexes published previously,[35] where the intrinsic ^{15}N chemical shifts refer to the value of 268 ppm of neat frozen 2,4,6-trimethylpyridine. The solid correlation curve in Figure 3b was calculated as described in the Theoretical Section from eq 3, using a limiting ^{15}N chemical shift of the hypothetical "free" pyridinium nitrogen at −140 ppm. This value was obtained by fitting the correlation curve to the experimental data points in Figure 3b. The dashed line was calculated using a value of −130 ppm proposed previously for 2,4,6-trimethylpyridine−acid complexes.[35,40] We associate the small difference in the limiting values to the influence of the chemical structure. Thus, using the solid line in Figure 3b, we were able to derive values of r_{HN} or r_{DN} for **1** and **2** from the corresponding intrinsic ^{15}N chemical shifts even in the cases where these distances could not be obtained by dipolar NMR. Note that, in this correlation, we neglect the difference between cubic and mean average distances. As discussed in the Experimental Section, the error on r_{HN} or r_{DN} increases when its value is increased. Assuming linear hydrogen bonds and proceeding as described previously in this paper for **1g**-*d* and **1j**-*d*, the corresponding values of r_{OH} were estimated from the correlation curve in Figure 3a. These are presented in Table 3.

2. HN Distance− ^{15}N Chemical Shift Correlation of the Intramolecular O2H2N2 Hydrogen Bond. The solid state NMR spectra described above indicate that the proton in the intramolecular OHN hydrogen bond is located near oxygen in crystalline **1b**, **1f**, and **2a** but near nitrogen in **2c**. No signs of a tautomerism between an OH and a HN form (Scheme 3) were observed, as is usually found for these types of molecules in the liquid state.[20] Therefore, we did not need to take this tautomerism into account in estimating the HN distances of the intramolecular O2H2N2 hydrogen bonds of **1** and **2** by NMR. We proceeded in a similar way as discussed in the preceding sections for the intermolecular O1H1N1 hydrogen bond, that is, estimated the hydrogen bond geometries by using a similar correlation curve as that depicted in Figure 3b. The difference was that we used the limiting chemical shift value of −158 ppm for the protonated nitrogen (see eq 3), which was estimated previously for the intramolecular O2H2N2 hydrogen bond of a model Schiff base.[20] The distances obtained are included in Table 3; a plot of the corresponding correlation curve is presented in the Supporting Information. Table 3 also includes the intramolecular heavy atom distances, r_{ON}, estimated using a hydrogen bond angle α(O2H2N2) $\approx$ 150°. This value was estimated from X-ray diffraction,[46] which may exhibit a systematic error.

B. Comparison between Distances Obtained by Diffraction Methods and by Solid-State NMR. The known X-ray crystallographic structures[1,2,4,11,12,46] of PLP, PL, and PN and the neutron structure of PN·HCl are depicted in Figure 5. Figure 6 contains the X-ray crystallographic structures of the model Schiff bases **1** and **2** and their acid-base adducts. Some hydrogen bond distances obtained here by solid state NMR are included for comparison.

1. PLP and Its Analogues. PLP in the hydrated form (Figure 5a) forms an intermolecular O1H1N1 hydrogen bond between the pyridine ring and the side-chain phosphate group of an adjacent molecule, exhibiting a N1···O1 distance of 2.671(6) Å.[4] We predict by ^{15}N NMR a value of $r_{HN} = 1.08$ Å for the intermolecular O1H1N1 hydrogen bond and a value of $r_{ON} \cong r_{OH} + r_{HN} \approx 2.68$ Å, which is close to the crystallographic value. It is tempting to associate this coincidence to the presence of a linear hydrogen bond. It follows that neutral PLP exhibits a zwitterionic structure, where the proton comes from the phosphate group which still carries a remaining proton.

The crystal structure[11] of PL in the cyclic hemiacetal form is presented in Figure 5b. The crystal packing shows an intermolecular O1H1N1 hydrogen bond between the pyridine ring and the phenolic group of a neighboring molecule, exhibiting an N1···O1 distance of 2.669(1) Å.[11] By NMR, the distances $r_{HN} = 1.06$ and $r_{OH} + r_{HN} = 2.73$ Å were obtained. The latter is larger than the distance r_{ON} obtained from X-ray diffraction. A

Table 3. Comparison of X-ray and NMR Crystallographic Data of the Inter- and Intramolecular OHN Hydrogen Bonds

	Crystallographic Values				NMR Values		
Intermolecular O1H1N1 Hydrogen Bond	r_{HN}/Å H1···N1	r_{OH}/Å O1···H1	r_{ON}/Å O1···N1	α(OHN)/° O1···H1···N1	r_{HN}[h]/Å H1···N1	r_{OH}[h,i]/Å O1···H1	r_{ON}[h,i]/Å O1···N1
PLP/analogue:							
PLP[a]	0.92	1.76	2.671(6)	168	1.08	1.60	2.68
PN[b]	1.74	0.99	2.729(5)	177	1.55	1.06	2.61
PL[c]	0.93	1.74	2.669(1)	170	1.06	1.67	2.73
PM·2HCl[d]	0.84				1.08		
PN·×b0HCl[f]	1.040(8)				1.04		
aldenamine Schiff base:							
1b[e]	1.86	0.92	2.752(7)	162	1.71	1.01	2.74
1f[e]	1.01	1.55	2.549(3)	170	1.14	1.43	2.57
aldimine Schiff base:							
2a[e,g]	1.95	0.92	2.865(2)	171	1.88	0.99	2.86
2c[e]	0.95	1.71	2.614(2)	160	1.12	1.47	2.59
Intramolecular O2H2N2 Hydrogen Bond	r_{HN}/Å H2···N2	r_{OH}/Å O2···H2	r_{ON}/Å O2···N2	α(OHN)/° O2···H2···N2	r_{HN}[h]/Å H2···N2	r_{OH}[h,i]/Å O2···H2	r_{ON}[h,i]/Å O2···N2
aldenamine Schiff base:							
1b[e]	1.71	1.01	2.545(6)	140	1.68	1.02	2.55[k]
1f[e]	1.69	0.95	2.553(3)	148	1.90	0.98	2.78[k]
aldimine Schiff base:							
2a[e,g]	1.73	0.92	2.570(2)	152	1.81	1.00	2.73[k]
2c[e]	0.93	1.81	2.595(2)	141	1.05	1.72	2.62[k]

[a] X-ray values obtained from ref 4. [b] X-ray values obtained from ref 1. [c] X-ray values obtained from ref 11. [d] X-ray values obtained from ref 12, the crystal structure is the mono hydrochloride. [e] X-ray values obtained from ref 46. [f] From neutron diffraction analysis.[2] [g] From the centrosymmetric dimer involving the side-chain hydroxyl group.[46] [h] NMR crystallographic values are extrapolated from the experimental isotropic ^{15}N chemical shifts. [i] $r_{OH} = r_{ON} - r_{HN}$. [j] $r_{NO} = r_{HN} + r_{OH}$. [k] Estimated by using α(OHN) obtained from X-ray analysis and calculated by using the law of cosines.

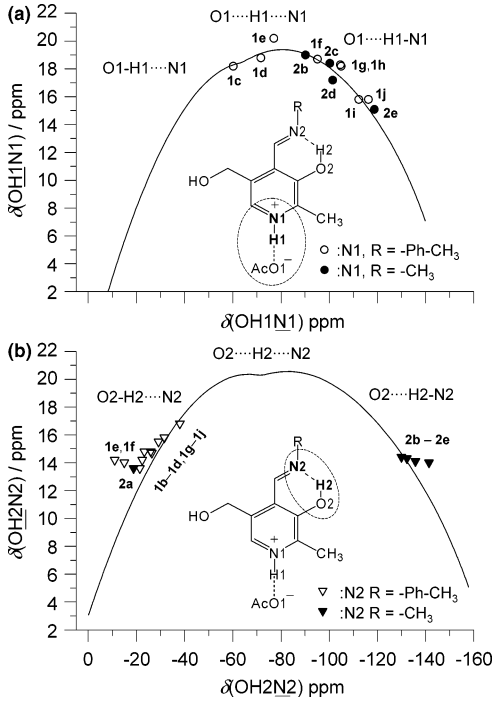

Figure 4. ^{1}H versus ^{15}N chemical shift correlations for the aldenamine Schiff base-adducts **1b**−**1j** and the aldimine Schiff base-adducts **2a**−**2e**. (a) The intermolecular O1H1N1 hydrogen bond. (b) The intramolecular O2H2N2 hydrogen bond. For the calculation of the curves, see text.

part of this difference arises probably from the margin of error of NMR, but the presence of a slightly nonlinear H bond is not excluded.

The crystallographic structure of PN[1] is shown in Figure 5c. PN forms an intermolecular O1H1N1 hydrogen bond between the pyridine ring and the side-chain hydroxyl group of an adjacent molecule, with a heavy atom distance of r_{ON} = 2.729(5) Å.[1] The sample studied by NMR was amorphous (see Figure S4 in the Supporting Information). A value of $r_{HN} \approx$ 1.55 Å was obtained by NMR, that is, $r_{OH} \approx$ 1.06 Å. The sum of the two distances, 2.61 Å, is smaller than the crystallographic value. We assign this difference to different structures of the amorphous and the crystalline forms. We note, however, that the proton in amorphous PN is located close to the oxygen in the intermolecular O1H1N1 hydrogen bond.

The neutron structure of PN·HCl (Figure 5d) exhibits a r_{HN} distance of 1.040(8) Å.[2] From the ^{15}N chemical shift of PN·HCl, we obtained the same value of r_{HN} = 1.04 Å, which indicates the reliability of the NMR method.

We performed some preliminary NMR experiments on PM and its dihydrochloride (PM·2HCl), see Scheme 1 and Tables 1 and 3. The interested reader can find the results and discussion in the Supporting Information.

2. Aldenamine and Aldimine Model Schiff Bases 1 and 2. The aldenamine Schiff base **1b** (Figure 6a) forms intermolecular O1H1N1 hydrogen-bonded chains involving the hydroxyl side groups and the pyridine rings of adjacent molecules, exhibiting a N1···O1 distance of 2.752(7) Å.[46] For the intramolecular O2H2N2 hydrogen bond, a heavy atom distance of 2.545(6) Å was reported.[46] We estimated, by NMR, a r_{HN} distance of 1.71 Å and a r_{ON} distance of 2.74 Å for the intermolecular O1H1N1 hydrogen bond, where the proton is located on the oxygen of the neighboring hydroxyl group. In the intramolecular O2H2N2 hydrogen bond, the proton is located near the oxygen atom, as inferred by the estimated r_{HN} distance of 1.71 Å from NMR. This is expected for an enolimine form of the Schiff base.

The structure of the aldenamine **1b**−2-nitrobenzoic acid adduct (**1f**) is depicted in Figure 6b. The O1···N1 distance of the intermolecular O1H1N1 hydrogen bond between the carboxylic group and the pyridine ring in **1f** is 2.549(3) Å.[46] A similar r_{ON} distance for **1b** of 2.553(3) Å was found for the intramolecular O2H2N2 hydrogen bond.[46] The estimated r_{HN} distance of 1.90 Å by NMR shows that the Schiff base is still

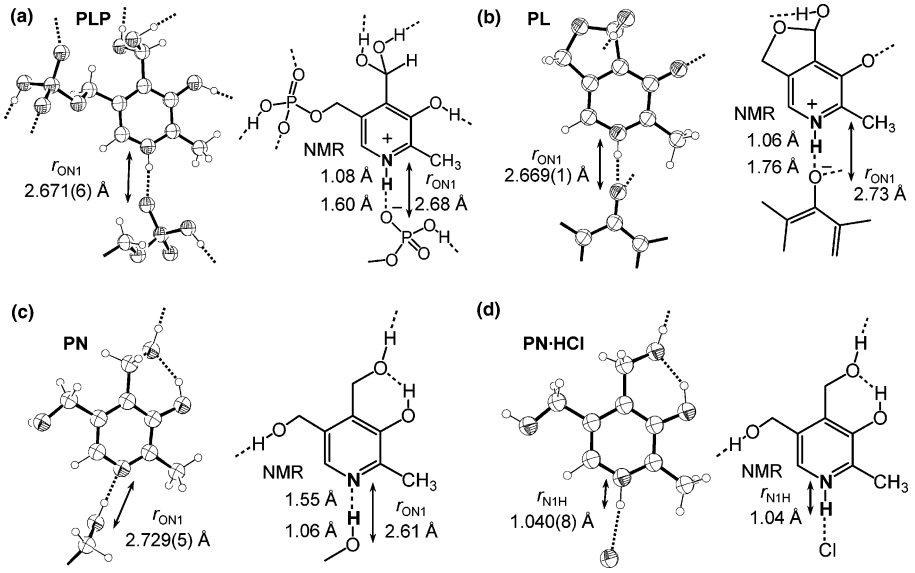

Figure 5. Crystallographic structures of PLP and its analogues. X-ray diffraction adapted (a) for PLP (hydrate form) from ref 4, (b) for PL (hemiacetal) from ref 11, and (c) for PN from ref 1. (d) Neutron diffraction adapted for PN·HCl from ref 2. The parameters shown are listed in Table 3.

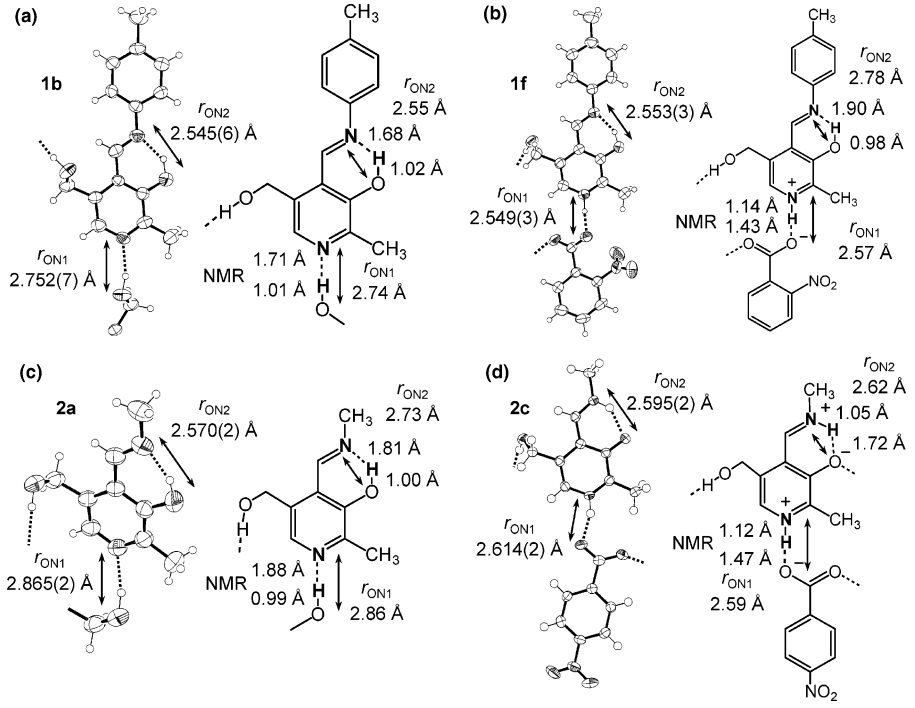

Figure 6. Crystallographic structures of (a) the aldenamine Schiff base (**1b**), (b) **1b**−2-nitrobenzoic acid (**1c**), (c) the aldimine Schiff base (**2a**), and (d) **2a**−4-nitrobenzoic acid (**2c**) obtained by X-ray diffraction, adapted from ref 46. The parameters are listed in Table 3.

in the enolimine form. Therefore, the bonding in the intramolecular O2H2N2 hydrogen bond is not altered compared to that in **1b**. However, the pyridine ring is now involved in an intermolecular O1H1N1 hydrogen bond with the carboxylic group of the acid added. NMR predicts a r_{HN} distance of 1.14 Å and a r_{ON} distance of 2.57 Å, which are in agreement with X-ray diffraction. This represents a substantial compression of the heavy atom r_{ON} distance compared to that of the weaker intermolecular O1H1N1 hydrogen bonds of **1b**. The proton is located near the ring nitrogen N1, leading to a zwitterionic structure.

The X-ray structure of the aldimine Schiff base **2a** is depicted in Figure 6c. Compound **2a** is packed as cyclic centrosymmetric dimers, involving intermolecular O1H1N1 hydrogen bonds between the hydroxylic side group and the pyridine rings. The O1···N1 distance is 2.865(2) Å, which is substantially larger than in the corresponding chains of **1b**.[46] Also, a O2···N2 distance of 2.570(2) Å was reported for the intramolecular O2H2N2 hydrogen bond.[46] The basicity of the CH_3−N group is expected to be larger than that of the corresponding tolyl−N group in **1b**. A N2···H2 distance of 1.81 Å was estimated for the proton in the intramolecular O2H2N2 hydrogen bond by NMR. The proton remains on the oxygen atom, giving an enolimine form. Also, we can predict, by NMR, an H1···N1 distance of 1.88 Å and an O1···H1 distance of 0.99 Å for the intermolecular O1H1N1 hydrogen bond of **2a**. This shows that

the proton remains on the hydroxyl group in the packed cyclic centrosymmetric dimers of **2a**.

The crystal structure of the aldimine **2a**−4-nitrobenzoic acid adduct (**2c**) is depicted in Figure 6d. As in **1f**, an acid−base complex exhibiting an intermolecular O1H1N1 hydrogen bond between the carboxylic group and the pyridine ring is formed. Again, the O1···N1 distance is quite short at 2.6142(2) Å, and the intramolecular O2···N2 distance is 2.595(2) Å.[46] By NMR, a O1···H1 distance of 1.47 Å and a H1···N1 distance of 1.12 Å are estimated, which is in agreement with the crystallographic value; however, the presence of a zwitterionic structure is demonstrated. As compared to that of **2a**, the intramolecular O2H2N2 hydrogen bond is substantially altered. The protonation of the pyridine nitrogen leads to a shift of the proton in the intramolecular O2H2N2 hydrogen bond, entirely stabilizing the ketoamine form. This is evidenced by a shorter H2···N2 distance of 1.05 Å, predicted by NMR. Hence, using NMR, the coupling of the intra- and intermolecular OHN hydrogen bonds is clearly demonstrated.

C. ^{1}H−^{15}N Chemical Shift Correlations and Geometric Coupling of the Inter- and Intramolecular OHN Hydrogen Bonds. We are now in a position to discuss the evolution of the NMR parameters and hydrogen bond geometries of the two functional OHN hydrogen bonds in the series of the Schiff bases **1** and **2**, which can be regarded as snapshots of a coupled double-proton transfer. Instead of representing the data in terms of a correlation diagram such as Figure 3a, we translate the correlation curve $q_2 = r_{OH} + r_{HN}$ versus $q_1 = 1/2(r_{OH} - r_{HN})$ into the corresponding NMR parameter curve, that is, the chemical shift of the H-bonded proton δ(O$\underline{H}$N) as a function of the ^{15}N chemical shift δ(OH$\underline{N}$). This correlation is expressed implicitly by eqs 3 and 4. It arises from the observation that the ^{15}N chemical shifts are measures of the proton positions q_1 in the hydrogen bonds, while the ^{1}H chemical shifts are measures of the sum, q_2, of the O···H and H···N distances.[40] Such correlations have been observed previously for pyridine− and 2,4,6-trimethylpyridine−carboxylic acid complexes in the solid and liquid states.[35−40] For a clearer comparison of different hydrogen bonds, it is convenient to reference the ^{15}N chemical shifts not to a standard such as ammonium chloride but to the value of the nitrogen atom in a non-hydrogen-bonded form, that is, to **1a** for the pyridine-type nitrogen atoms and to the methoxy-substituted Schiff base *N*-(2-methoxybenzylidene)methylamine.[20]

The results for the intermolecular and the intramolecular OHN hydrogen bond of **1** and **2** are depicted in Figure 4. As described in the theoretical section, the parameters used to calculate the solid lines are the same as those used to calculate the hydrogen bond correlation in Figure 3a and the NMR chemical shifts of the hypothetical limiting states listed in Table 4. Here, δ(N$\underline{}$)^o represents the limiting chemical shift of the hypothetical free nonprotonated nitrogen, and δ(O$\underline{H}$)^o is that of the free OH group, while δ(H$\underline{N}$)^o and δ(H$\underline{N}$)^o represent the chemical shifts of the separate O^- and HN^+ moieties. Additionally, δ(O$\underline{H}$N)* and δ(OH$\underline{N}$)* are excess terms that describe the deviations of the chemical shifts of the quasisymmetric strongest hydrogen bonds from the average of the hypothetical limiting molecular moieties.

The chemical shift parameters for the intermolecular hydrogen bond were those reported previously[40] for 2,4,6-trimethylpyridine-acid complexes in the solid state. The chemical shift parameters for the intramolecular hydrogen bond were taken partially from those reported previously for the model Schiff base *N*-(3,5-dibromosalicylidene)methylamine, with adaptation by fitting to the experimental data points in Figure 4b. We associate the small difference with the influence of the chemical structure of the Schiff bases since it is known that Schiff bases containing different substituents exhibit different ^{15}N chemical shift values.[94] For example, Naulet et al. observed a difference of 4 ppm,[95] which was used for imines that carry a phenylic or aliphatic group.

Table 4. Parameters for the NMR Hydrogen Bond Correlations of the Schiff Bases

	δ(N$\underline{}$)^o /ppm	δ(HN$\underline{}$)^{oc} /ppm	δ(OHN$\underline{}$)* /ppm	δ(O$\underline{H}$)^o /ppm	δ(H$\underline{N}$)^o /ppm	δ(OH$\underline{N}$)* /ppm
O1H1N1[40,a]	0	−140	0	−3	7	20
O2H2N2[20,b]	0	−158	−5	3	5	20

[a] The ^{15}N chemical shifts of the intermolecular O1H1N1 hydrogen bond are referenced to solid **1a**, resonating at 282.5 ppm with respect to solid $^{15}NH_4Cl$. [b] The ^{15}N chemical shifts of intramolecular O2H2N2 hydrogen bond are referenced to the methoxy-protected Schiff base,[20] resonating at 276 and 280 ppm for the **1** and **2**, respectively, with respect to solid $^{15}NH_4Cl$.[94,95] [c] δ(H*N*)^o was obtained by fitting the correlation curve to the experimental data points.

The solid correlation curves in Figure 4 give an acceptable fit to the experimental data. The curves are similar to the q_2 versus q_1 curve of Figure 3a. The difference is that this curve has no ends since q_1 and q_2 can be infinite. In contrast, the ^{1}H/^{15}N chemical shift correlation curve has limiting values since the chemical shifts of the separate moieties eventually become independent of internuclear distance. Nevertheless, in the regions where hydrogen bonds exist, both correlation curves display a similar behavior, and one can discuss the data points in Figure 4 in terms of the geometric changes indicated in Figure 3a.

Different hydrogen bond geometries are obtained depending on the acidity of the proton donor interacting with the pyridine ring of the Schiff base. In contrast to collidine−benzoic acid complexes,[40] which form molecular complexes of the type O−H···N, we could not obtain such a structure for solids **1** and **2**, but rather, strongly hydrogen-bonded complexes of the type $O^{\delta-}\cdots H\cdots N^{\delta+}$ or zwitterionic salts, $O^-\cdots H-N^+$, were obtained. The former exhibit low values of q_2 (<2.6 Å) and low-field ^{1}H chemical shifts in the range of 20 ppm.[40] In the zwitterionic states, the values of q_2 increase according to Figure 3a leading to a decrease of the ^{1}H chemical shifts, as illustrated by the solid line in Figure 4a.[35,40]

For the aldenamine Schiff base-acid adducts **1**, comparison of Figure 4a and 4b indicates that, when the proton is shifted from the benzoic acid oxygen to the pyridine nitrogen, the intramolecular hydrogen bond is shortened in the series **1b**−**1j**, but its hydrogen bond proton remains closer to oxygen than to nitrogen. Because of the small low-field ^{15}N chemical shift, **1e** to **1f** are somewhat located outside of the correlation curve (Figure 1). These deviations are, however, so small that their interpretation is difficult at present.

By contrast, the aldimine Schiff base adducts, **2**, behave differently; the formation of a hydrogen-bonded complex with the pyridine nitrogen immediately shifts the proton in the intramolecular hydrogen bond from oxygen to nitrogen, forming the zwitterionic state $O2^{\delta-}\cdots H2-N2^{\delta-}$. Neither an intermediate

(94) Neuvonen, K.; Fueloep, F.; Neuvonen, H.; Koch, A.; Kleinpeter, E.; Pihlaja, K. *J. Org. Chem.* **2003**, *68*, 2151−2160.
(95) Naulet, N.; Martin, G. J. *Tetrahedron Lett.* **1979**, *17*, 1493−1496.

state nor tautomerism between two protonation states was observed, as was found with other Schiff bases in solution.[20,28−33]

The origin of the H/D isotope effects on the ^{15}N chemical shifts of pyridine derivative-acid complexes,[35−37,40] which exhibit an intermolecular hydrogen bond, and of the model Schiff base *N*-(3,5-dibromosalicylidene)methylamine,[20] which has an intramolecular hydrogen bond, has been discussed recently. The latter is influenced by intrinsic effects arising from isotope effects on the hydrogen bond geometry and by equilibrium isotope effects on tautomerism.[20] However, the values that we have obtained here for the intramolecular H bond in the solid state (cf. Table 1) are not precise enough for a detailed discussion. Nevertheless, fair agreement is found with the values obtained for the intermolecular H-bonds in complexes of 2,4,6-trimethylpyridine with various acids (Table 2).[35,40] A plot of these isotope effects as a function of the ^{15}N chemical shifts is presented in Figure S7 in the Supporting Information.

D. The pK_a Values and the Hydrogen Bond Geometries in the Solid State. Here, acid-base interactions in nonaqueous environments such as the solid state, aprotic polar solvents, or the interior of an enzyme are addressed. Usually, the strength of an acid in aqueous solution is expressed by its pK_a value defined by

$$AH_{aq} \overset{K_a^{AH}}{\rightleftharpoons} A^-_{aq} + H^+_{aq}$$

$$K_a^{AH} = \frac{[A^-_{aq}][H^+_{aq}]}{[AH_{aq}]},\ -\log K_a^{AH} = pK_a^{AH} = -\log [H^+_{aq}] = \text{pH for } [AH_{aq}] = [A^-_{aq}] \quad (6)$$

and

$$BH^+_{aq} \overset{K_a^{BH}}{\rightleftharpoons} B_{aq} + H^+_{aq}$$

$$K_a^{BH} = \frac{[B_{aq}][H^+_{aq}]}{[BH^+_{aq}]},\ -\log K_a^{BH} = pK_a^{BH} = -\log [H^+_{aq}] = \text{pH for } [BH^+_{aq}] = [B_{aq}] \quad (7)$$

Here, the acids and the bases all form hydrogen bonds to water molecules, but there is no direct acid-base interaction. The acid-base equilibrium is given by

$$AH_{aq} + B_{aq} \overset{K}{\rightarrow} A^-_{aq} + BH^+_{aq},\ K = \frac{[A^-_{aq}][BH^+_{aq}]}{[AH_{aq}][B_{aq}]} = \frac{K_a^{AH}}{K_a^{BH}} = 10^{(pK_a^{BH} - pK_a^{AH})} = 10^{\Delta pK_a} \quad (8)$$

By contrast, in nonaqueous environments, direct hydrogen bonds between the acid and the base are usual, for example, in the adducts of **1** and **2**. In this case, eq 8 is no longer valid. If there is an equilibrium between two forms such as

$$A`-H\cdots B \overset{K}{\rightleftharpoons} A`\cdots H-B^- \quad (9)$$

the equilibrium constant, *K*, characterizing the ratio of the two tautomeric forms is not the same as the one in water. This phenomenon is often incorrectly called a pK_a shift. Generally, direct acid-base hydrogen bonding may not lead to a conventional equilibrium between two forms, but it may lead to a given average hydrogen bond geometry; an increase in the acidity or proton donating power of the donor leads to a shift of the proton position from the donor to the acceptor along a correlation curve, such as depicted in Figure 3a. The hydrogen geometry obtained depends on the molecular structure, environment, and the local electric fields.[96] In other words, both the pK_a values and the hydrogen bond geometry are measures of acid-base properties of a proton donor−acceptor pair. It is, therefore, not astonishing that, for pyridine- and 2,4,6-trimethylpyridine-acid adducts, a near linear relation of pK_a with the proton-transfer coordinate q_1^H has been observed.[35,41]

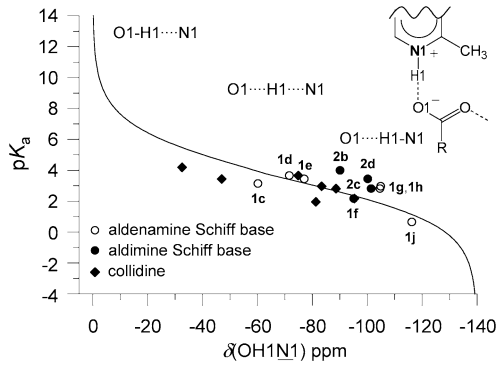

Figure 7. The pK_a values versus ^{15}N chemical shift correlation for the acid components in the organic solids of the aldenamine Schiff base-adducts **1b**−**1j** (open circles) and aldimine Schiff base-adducts **2b**−**2e** (filled circles). The diamonds represent the values for 2,4,6-trimethylpyridine−HA complexes[35] with respect to the frozen, bulk 2,4,6-trimethylpyridine. The pK_a values are a function of q_1^H, with the relation $pK_a = A - Bq_1^H$ (see eq 5), by using the parameters $A = 3.5$ and $B = 8$. For the calculation of the curve, see text.

Since the ^{15}N chemical shifts of intermolecular O1H1N1 hydrogen bonds in the absence of tautomeric equilibria are convenient experimental measures of q_1^H, we have plotted, in Figure 7, the pK_a values of the acids forming the solid adducts of **1** and **2** as a function of the pyridine ^{15}N chemical shifts (cf. Table 1). An alternative plot (cf. Figure S8) of the associated pK_a values as a function of the proton-transfer coordinate q_1^H is given in the Supporting Information. The solid line was calculated using eq 5, where the parameters were adapted in such a way to fit the experimental data points best; see Figure 7. However, the scatter in the data obscures any direct relation between the acidity in water and nonaqueous environments. Moreover, comparison of the solid adducts, **1e** and **2c**, with 4-nitrobenzoic acid and of **1g** and **2d** with 3,5-dinitrobenzoic acid does not clarify the relation. Whereas, in the first pair, the aldimine seems to be more basic than the aldenamine, they exhibit the same basicity in the second pair.

As mentioned previously,[35] eq 5 indicates that, in order to get a hydrogen bond with $q_1 = 0$, an acid with a pK_a value of ~3 is needed. Since the pK_a value of pyridinium is 5.23,[97] this indicates that these substituted pyridines are ~2 pK_a units more acidic than pyridinium, as has been shown previously for solid 1:1 complexes of benzoic acids with pyridine derivatives by IR spectroscopy.[35,98−101] A solid molecular complex of benzoic acid with pyridine can be obtained only with collidine, which is more basic than benzoate.[35] In contrast to that in the solid

(96) Ramos, M.; Alkorta, I.; Elguero, J.; Golubev, N. S.; Denisov, G. S.; Benedict, H.; Limbach, H. H. *J. Phys. Chem. A* **1997**, *101*, 9791−9800.
(97) Tamres, M.; Searles, S.; Leighly, E. M.; Mohrman, D. W. *J. Am. Chem. Soc.* **1954**, *76*, 3983−3985.

state, in aqueous solution, the large dielectric constant of water increases the acidity of a proton donor by favoring zwitterionic forms exhibiting large dipole moments. In nonaqueous solution, the acidity of a proton donor increases if it is involved in a hydrogen-bonded network such as AH··· $(AH···)_nAH$.[36] Since such association does not occur in water, the description of acidity in terms of a single pK_a value is not appropriate for nonaqueous systems.

Conclusions

Using ^{15}N CP MAS and ^{1}H MAS NMR, we have studied a series of specifically ^{15}N-labeled hydrogen-bonded solids modeling various forms (Schemes 1 and 2) of the cofactor pyridoxal-5′-phosphate (PLP) in enzymatic environments. In particular, Schiff base formation with an ϵ-amino group of a lysine side chain or with amino acids, as well as hydrogen bonding of the pyridine nitrogen to an aspartic acid residue, was modeled in the series of novel 1:1 hydrogen-bonded solid complexes **1** and **2**, some of whose crystal structures were obtained previously.[46] The geometries of the intermolecular O1H1N1 hydrogen bonds were estimated by establishing a correlation between nitrogen−hydrogen distances obtained by dipolar $^{15}N-^{2}H$ NMR and ^{1}H and ^{15}N chemical shifts and by well-established geometric OHN hydrogen bond correlations. The latter also helped to locate the proton in the intramolecular O2H2N2 hydrogen bond. However, no thermal tautomerism was observed for the latter in the solid state. When the acidity of the benzoic acids was increased, the proton shifted continuously from the carboxylate oxygen to the pyridine nitrogen, forming a zwitterionic state. During this process, hydrogen bond compression was observed, which is strongest in the quasisymmetric state where the proton is located in the hydrogen bond center.

While similar features of pyridine and its derivatives have been observed previously, the most important finding in this paper is the coupling of the proton transfer in the intermolecular O1H1N1 hydrogen bond to the proton transfer in the intramolecular O2H2N2 hydrogen bond. When the Schiff base nitrogen atom carries an aromatic substituent, protonation of the pyridine ring only increases slightly the O2···H2 bond length of the intramolecular O2H2N2 hydrogen bond and compresses the latter somewhat. However, whenever the Schiff base nitrogen atom of PLP carries an aliphatic substituent, as in the internal and external aldimines of PLP in the enzyme environment, protonation of the ring nitrogen also shifts the proton in the intramolecular OHN hydrogen bond from oxygen to the Schiff base nitrogen, which increases its positive electric charge. This charge on the Schiff base nitrogen may well be a prerequisite for enzyme activity, as proposed by Bach et al.[19]

Unfortunately, it was not possible to crystallize **2a** with a weak acid such as benzoic acid, which has a pK_a value similar to an aspartic acid side chain. If such a complex existed, from Figure 7, we would expect a structure where the protons in both the inter- and intramolecular OHN hydrogen bonds are close to oxygen, that is, that a zwitterionic structure will not be formed.

In the solid state, the coupled double-proton shift could be achieved by increasing the acidity of the benzoic acids via electron-withdrawing substituents. On the other hand, in the enzyme active site, the local polarity must be increased over the solid states studied here. Specific interactions of the aspartic acid residue with other proton/hydrogen bond donors is commonly observed in PLP enzyme structures, and increases in the local dielectric constant due to the protein structure (for example, α-helix macro dipoles) are probable. Combined, these effects as well as specific interactions of active-site residues with the Schiff base N and O make the pyridine ring and Schiff base N-protonated forms readily accessible. Currently, studies on the effects of the local polarity on the NMR parameters of the model Schiff bases are underway, the results of which will be reported elsewhere.

Acknowledgment. This work was supported by the Deutsche Forschungsgemeinschaft, Bonn, and the Fonds der chemischen Industrie, Frankfurt.

Supporting Information Available: The static powder ^{15}N spectra of the undeuterated and deuterated aldenamine Schiff base and its acid-base adducts as well as the theory of the dipolar ^{15}N solid-state NMR are presented. ^{15}N spectra and crystallographic structures for PLP and its analogues are presented. A plot of the isotopic effect, $^{1}\Delta N1(D)$, as a function of the ^{15}N chemical shifts, δ(O1H1N1), is given. A plot of the intramolecular r_{HN} distances against the ^{15}N chemical shift as well as the alternative correlation of the associated pK_a values with the proton-transfer coordinate q_1^H is given. This material is available free of charge via the Internet at http://pubs.acs.org.

JA066240H

(98) Majerz, I.; Malarski, Z.; Sobczyk, L. *Chem. Phys. Lett.* **1997**, *274*, 361−364.
(99) Wolny, R.; Koll, A.; Sobczyk, L. *J. Phys. Chem.* **1985**, *89*, 2053−2058.
(100) Hawranek, J. P.; Oszust, J.; Sobczyk, L. *J. Phys. Chem.* **1972**, *76*, 2112−2116.
(101) Johnson, S. L.; Rumon, K. A. *J. Phys. Chem.* **1965**, *69*, 74−86.